Spectroscopy of Transition Region Species

PHILIP R. BROOKS

Department of Chemistry and Rice Quantum Institute, Rice University, Houston, Texas 77251

Received April 20, 1987 (Revised Manuscript Received September 8, 1987)

Contents

Phil Brooks was born in Chicago on New Year's Eve 1938. He went West and did undergraduate research (on DNA!) with Norman Davidson at Caltech and received a BS in 1960. He worked with Dudley Herschbach on the "lunatic fringe" at the University of California, Berkeley, in the early 1960s, and received the PhD in 1964. During a short postdoctoral with Bill Lichten at Chicago, he was introduced to molecular beam deflection techniques, and employs those techniques to produce beams of oriented molecules. Since 1964 he has been at Rice University, where he is currently Professor. His research interests are currently the reactions of oriented molecules and spectroscopy during reactive collisions. He is a single parent to four children, and in his spare time he is an avid cyclist and home repair specialist.

During a chemical reaction event, old bonds dissolve and new bonds form. Transient species are formed that are *neither* reagents *nor* products, but instead are species *in transition* between reagents and products. The nature and time evolution of these transient species obviously carry an enormous amount of information about the chemical reaction. This article reviews methods being devised to spectroscopically probe these species.

I. Introduction

During a chemical reaction, reagents are transformed into products. The reaction event involves the breaking of old chemical bonds and the formation of new bonds on a short time scale. In the gas phase a rough estimate of this time scale is the time scale of a collision, $\approx 10^{-12}$ s, corresponding to the time required for a molecule of thermal speed ($\approx 10^4$ cm/s) to traverse a molecular diameter ($\approx 10^{-8}$ cm). The time scale for macroscopic bimolecular chemical reactions is usually much longer, not because the reaction event itself is slower, but because the frequency of collisions leading to a reactive event is lower and because only a small fraction of these collisions are successful in leading to reaction.

Understanding the dynamics of the reaction event itself is the goal of chemical dynamics. It is the reaction event, the sum of processes that occur during the collision, that is of fundamental chemical interest, but because this event occurs on such a short time scale, direct observation has previously not been possible. Most of our information regarding the reaction event comes from experiments in which either the appearance of products or the disappearance of reactants is measured. These measurements on the asymptotic states of the chemically reactive system are usually combined with theory to work backward (or forward) to *infer* what takes place during the reaction event itself. This procedure has been remarkably informative, but it is nonetheless fraught with peril. Not only must the experimental observations be reliable and sufficiently accurate, but the theory used to extrapolate the data into the domain of the reactive event must also be appropriate. Unfortunately, clear-cut criteria for what constitutes "sufficiently accurate" data and "appropriate" theories are not readily available, and one must be content with rather tentative inferences about the reaction dynamics. But these tentative inferences

0009-2665/88/0788-0407$06.50/0

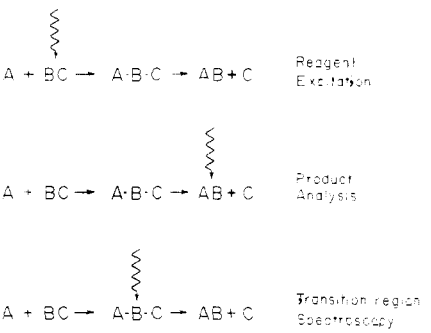

Figure 1. Schematic comparison of different ways light can interact with a chemically reactive system. (Top) The photon is resonant with an asymptotic energy difference in one of the *reagents*, and the effect on the reaction of reagent excitation will be studied. (Middle) The photon is resonant with an asymptotic energy difference in one of the *products*, and the quantum states of the product can be probed, usually as laser-induced fluorescence. (Bottom) The photon is *not* resonant with an asymptotic energy difference in either reagent or product, but may be resonant with a species *intermediate* between reagent and product, and absorption by this species forms the basis for "transition region spectroscopy".

are like threads: even though one may be weak, a large number can be woven into a durable cloth. Likewise our present understanding of chemical dynamics is woven from a large body of interdependent experimental and theoretical results.

Current laser and molecular beam studies are refining and extending our understanding of chemical reactions by interrogating the states of the reagents or the states of the products on a state-by-state basis (or even on a *state-to-state* basis).[1] But even these refined measurements are made in the asymptotic channels of the reaction and still require the reaction event itself to be reconstructed. Recently, however, several groups have sought to eliminate or reduce this reconstruction by developing techniques whereby reactions can be probed *during* the reactive process. By virtue of the time scale involved, these techniques are spectroscopic in nature, and have led to what has become known, for better or for worse, as "transition state spectroscopy".

In this review, we discuss the spectroscopy of real, transient species intermediate between reagents and products (i.e., of species *in transition*). We will refer to these as *transition region species* to emphasize that these encompass all nuclear configurations through which the system passes during the transition from reagents to products. (The various subgroups of nuclear configurations called "the transition *state*" in theories of chemical reaction rates are thus included in this definition.) Observations on the system *during* reaction, rather than in the asymptotic channels, are clearly a *new kind* of information, and thus have the possibility of giving new insight into an old problem.

A. Scope of Review

In this review we shall be concerned with the experimental aspects of the spectroscopy of molecules *during* reaction, otherwise known as "transition state spectroscopy" or "laser-assisted chemistry". Previous reviews include ref 2–4. We shall exclude from consideration those processes where lasers are used to prepare reagents in specified initial states[1,5] or where lasers are used to analyze the states of the products.[6] These distinctions may be more clearly made by reference to Figure 1. Here we show schematically photons interacting with reagents, with products, and finally with some kind of species *intermediate* between reagents and products called a *transition region species*. We anticipate many different configurations in the transition region in any given chemical reaction, but, aside from the nature of this distribution of states, we expect the spectroscopy of these species to be very similar to that of normal molecules.

TABLE I. Observations on Reactive Transition Region Species

reagents	products	detected as	ref
Light Absorbed by a Transition Region Species			
$K + HgBr_2 + h\nu$	$KBr + HgBr^*$	fluorescence of $HgBr^*$	9
$K + NaCl + h\nu$	$KCl + Na^*$	fluorescence of Na^*	10a,b, 11
$Hg + HgBr + h\nu$	$HgBr^* + ?$	fluorescence of $HgBr^*$	12
$Mg + H_2 + h\nu$	$MgH + H$	LIF of MgH	13a,b
$Na^* + Li + h\nu$	$NaLi^+ + e^-$	$NaLi^+$	14a,b
$Xe + Cl + h\nu$	$XeCl^*$	fluorescence of $XeCl^*$	15a,b, 16
$Xe + Br + h\nu$	$XeBr^*$	fluorescence of $XeBr^*$	17
Light Emitted by a Transition Region Species			
$F + Na_2$	$NaF + Na^*$	fluorescence of $(NaFNa)^*$	18a,b
$O_3 + h\nu$	$O_2 + O$	fluorescence of $O_2 \cdots O$	4, 19
$CH_3I + h\nu$	$CH_3 + I$	fluorescence of $CH_3 \cdots I$	4, 20
$NO_2 + h\nu$	$NO + O$	fluorescence of $NO \cdots O$	21

As will be discussed later, we expect laser interactions with a reactive system to be in the "weak-field" limit, even though the laser power may be high by conventional standards. Because our emphasis will be in using light to *probe* the chemical reaction, we will not emphasize recent theoretical work[7] concerned with very high laser intensities ($>10^8$ W/cm^2). At these high intensities, the laser field is expected to distort the molecular potential energy surface and thus *alter* the dynamics of the collision. While these effects are of considerable interest, studies have largely been restricted to nonreactive collisions,[8] and experimental observations of laser-altered chemical reactions have not, to our knowledge, been reported. We expect that experiments to probe chemical reactions at extremely high intensities will be enormously complicated by various other processes, such as multiphoton processes, which will compete with, and possibly obscure, the chemical reaction.

II. Overview

The spectroscopy of reacting systems is simultaneously new and old. There are similarities with, as well as differences from, other phenomena, especially with line broadening, and we would like to compare and contrast the spectroscopy of transition region species with various line-broadening effects. Before doing that in detail, however, it seems worthwhile to present an overview of the chemically reactive systems, which will be discussed in some detail below.

The chemical reactions for which studies have been reported are summarized in Table I. Very broadly speaking, the evidence for observation of species in the process of reacting is indirect: The system behaves *as if* a transition region species were absorbing (or emitting) the light. The experimental evidence, discussed in detail in section IV, is often the observation of a chemical reaction concomitant with the absorption or emission by a species which is *neither* reagent *nor* product. Even though such evidence may be regarded as indirect (and in some instances nonunique), the experiments represented in Table I nevertheless collectively offer evidence that transition region species can

TABLE II. Categories of Radiation–Collision Interactions

characteristics	species involved in transition: one	two	multiple
species undergoing change	A	(A + B)	(A B C)
light intensity	any (low)	high (MW/cm^2)	moderate (kW/cm^2)
photon energy[a] ($h\nu$)	$\Delta E_0 + \epsilon$	$E_A + E_B + \epsilon$	ΔE_{ABC}
examples	optical collision	radiative collision	"transition Region spectroscopy
	line broadening	LICET	
	redistribution	RAIC	"Laser-Assisted chemistry
	collision–induced transitions		

[a] The unperturbed transition in A occurs in the zero-pressure limit, where $h\nu = \Delta E_0$, the energy level separation in the isolated species. E_A and E_B refer to energies of the isolated species; ΔE_{ABC} refers to an overall energy change in the collision. Other symbols and abbreviations are discussed in the text.

be observed spectroscopically.

III. Background

Before discussing the absorption or emission of light during a chemical reaction event, it is useful to consider similar optical–collision processes that occur in the absence of chemical reaction. Some of these processes, such as those responsible for the broadening of atomic resonance lines,[22] are well-known, whereas others are not so well-known. These processes are instructive to consider because they introduce some useful concepts and terminology.

In Table II we have tried to categorize radiation–collision events of the type[23]

$$A + B^* \rightarrow C + D + h\nu$$

according to whether the photon is resonant (or nearly resonant) with a difference in energy levels in *one* species A, in *two* species A and B, or in *three* (or more) species A, B, and C.

A. One-Species Transitions

In such an event, the photon is (nearly) resonant with the energy difference between two eigenstates of one species, either an atom or a molecule, and any difference in energy, ϵ, is made up by the kinetic energy of the collision. There are two subcategories, according to whether, in the absence of collisions, the transition is allowed or forbidden.

1. Forbidden Transitions

If the transition is *forbidden*, the collision may relax some selection rule, and the transition would be observed at the resonance frequency,[24] ν_0, where

$$h\nu_0 = E_A^u - E_A^l = \Delta E_A \quad (1)$$

This is the phenomenon of *collision-induced emission or absorption* and was first observed[25] in the infrared absorption spectra of O_2 and N_2 with path lengths $\simeq$ 85 cm at pressures $\simeq$ 10 atm. The transition that is newly allowed by the collision still connects two states of a single stable species.

Experiments similar in spirit were reported by Su, Bevan, and Curl.[26] They irradiated a Cs gas cell containing a few Torr of rare gas with the output of a nitrogen-pumped dye laser tuned in the range 14 800–16 200 cm^{-1} and monitored the emission. *New lines* appeared in the fluorescent excitation spectrum when the rare gas was added. These lines correspond to allowed, unperturbed transitions in atomic Cs between the *excited* 5d $^2D_{5/2}$ state and various np $^2P_{3/2}$ and nf ^2F states. The authors suggested that the excited 5d $^2D_{5/2}$ state was formed (via an otherwise forbidden transition from the ^2S ground state) by absorption of a CsRg molecule *during* collision. (Excitation of the high Rydberg states was confirmed by observing fluorescence in the ultraviolet.) The probability of forming the 5d state depended on the added rare gas, usually being much greater for argon than for He.

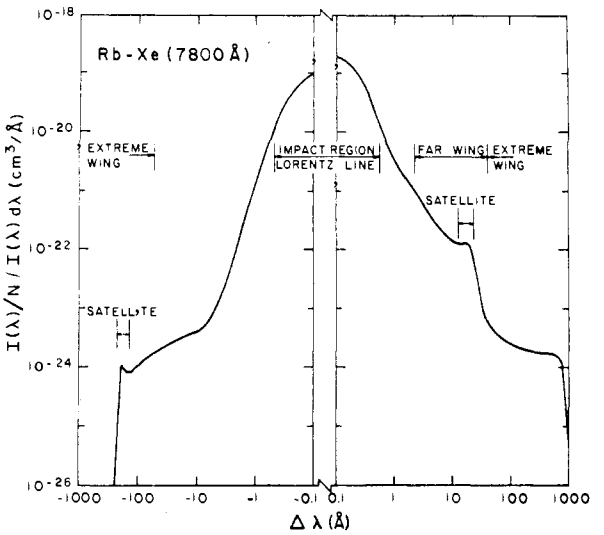

Figure 2. Normalized emission spectrum of Rb(5 $^2P_{3/2}$) perturbed by xenon. Note the double-logarithmic scale used to represent data over several orders of magnitude intensity. Also note that "impact" region, or line "core", results from very gentle collisions. Hard collisions greatly perturb the emitter and are represented by emission in the wings. (Reference 30, with permission.)

2. Line Broadening (Allowed Transitions)

If the transition is *allowed*, the collision can interfere with the absorption process and the line appears broadened. To gain some familiarity with various aspects of collision broadening, we discuss the *emission* of the Rb atom perturbed by collisions with xenon, which has been the subject of extensive investigations by Gallagher and co-workers.[27]

In the absence of collisions, the line width, $\Delta\nu$, is determined by the uncertainty principle to be $\Delta\nu = 1/\tau$, where τ is the lifetime of the upper state. For an allowed transition in the visible such as the $^2S \leftarrow {}^2P$ transition in Rb at 780 nm, $\tau \approx 10$ ns and $\Delta\nu \approx 100$ MHz ($\Delta\nu \approx 0.003$ cm^{-1}; $\Delta\lambda = 0.002$ Å), so the unperturbed line is indeed sharp. In the presence of collisions, however, the line is broadened and is schematically illustrated in Figure 2. The central portion of the line is not shown, but the intensity at the line center

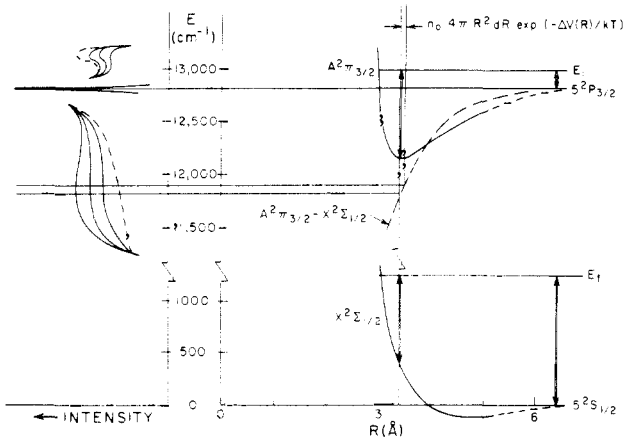

Figure 3. Model potentials showing Franck–Condon transitions from the upper A state (for Rb–Xe) to the very weakly bound X state. An increase in temperature in the colliding system decreases the probability the emitter is found in the region dR, and as shown on the left, the intensity of the wing *decreases* with temperature. (Reference 30, with permission.)

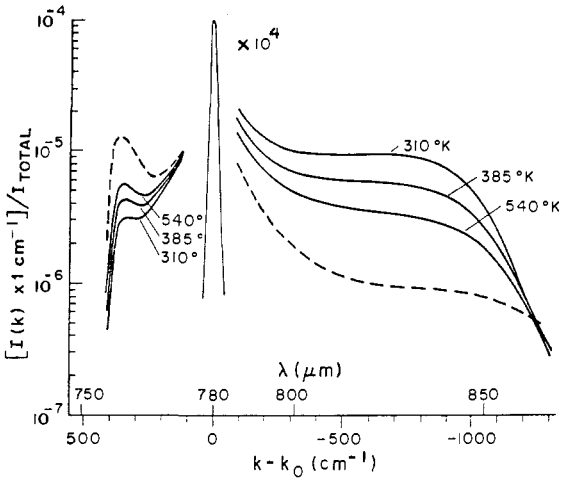

Figure 4. Normalized emission spectrum of the Rb 7800-Å D line perturbed by xenon at 10^{19}/cm^3 density. The gas temperature is indicated. Note that the red wing decreases in intensity at higher temperatures, which is opposite to the behavior in the blue wing. This shows that the red and blue wings arise from different states. (Reference 30, with permission.)

may rise several orders of magnitude, depending on the natural lifetime, unresolved hfs, etc.[28] We emphasize that the line is *still rather sharp*, and the effects of collisions are manifested mainly in the wings, where the intensity falls *rapidly* (note the logarithmic scale) with the detuning $\Delta\lambda = \lambda - \lambda_\infty$, where λ_∞ is the wavelength corresponding to the transition with the collision partners at infinite separation. The intensity as a function of detuning has been very carefully measured by Gallagher and co-workers in cells containing $\approx 10^{-6}$ Torr of Rb and several hundred Torr of Xe.

As indicated in Figure 2, it is convenient to divide the line into various regions:

(1) The "impact region", or "line core",[29] is characterized by frequencies $\Delta\nu \ll 1/\tau_c$, where τ_c is the duration of a collision, $\approx 10^{-12}$ s. These collisions are long-range van der Waals type collisions which perturb the emitter only *slightly*. Only limited information may be gleaned experimentally about the molecular potentials in this region.

(2) The "far-wing" and "extreme-wing" regions are characterized by $\Delta\nu \gg 1/\tau_c$. Collisions responsible for detunings in these regions are collisions of shorter range where the details of the potentials are important. In both regions, the line width depends on perturber pressure, and in the extreme wing the line shape also depends on the temperature. These regions are usually interpreted in terms of the quasi-static theory described below.

(3) The "satellite regions", described below, constitute a third region.

3. The Quasi-Static Theory (QST)

The QST regards the emitter–perturber system as a diatomic molecule that undergoes a transition from an upper state with a potential $V^*(R)$ to a lower state, characterized by $V(R)$. According to the classical Franck–Condon principle, the transition occurs rapidly in comparison to the nuclear motion, so the transition occurs at fixed R, and the frequency is given by

$$h\nu = V^*(R) - V(R) = \Delta V(R) \qquad (2)$$

A transition in the range $\nu \rightarrow \nu + \delta\nu$ from the upper state thus occurs while the nuclei are at separations in the range $R \rightarrow R + dR$, as suggested in Figure 3. A single collision event or state will thus yield a contribution to the intensity in the range $\nu \rightarrow \nu + \delta\nu$ *proportional to the time spent* in the range $R \rightarrow R + dR$ shown in Figure 3. The total intensity in this frequency range is then proportional to the average over all collision events, and the intensity at ν is given equivalently[28] by

$$I(\nu) \propto 4\pi N(R)[R(\nu)]^2[d\nu/dR(\nu)]^{-1} \qquad (3)$$

where $N(R)$ is the perturber density at R. In the far-wing region, $N(R) \approx N$ so the wing intensity is only dependent on N. In the extreme-wing region (characterized by *closer* collisions), $N(R)/N$ depends *also* on the temperature since the perturber is expected to be in statistical equilibrium with the emitter

$$N(R)/N = g_i/g_a \exp(-[V_i(R) - V_i(\infty)]/kT) \qquad (4)$$

where g_i and g_a are the molecular and atomic degeneracies, and $V_i(R) = V^*(R)$ in emission.

The "satellites" of Figure 2 arise from extrema in the difference potential, $\Delta V(R)$, since a range of R values can then correspond to a narrow frequency range, and $d\nu/dR(\nu) \rightarrow 0$ in eq 3. (Another extremum occurs in the asymptotes as $R \rightarrow \infty$ where ΔV is constant and the "satellite" is the resonance line.)

The line shape allows one to determine only the *difference* potential from eq 2, but the temperature dependence of the line shape allows one to determine $V^*(R)$ (or $V(R)$ in absorption experiments.) The emission spectrum of the Rb–Xe system has been measured at various temperatures by Gallagher and co-workers and is shown in Figure 4. The red wing shows a strong temperature dependence, and the blue wing shows a satellite, but the temperature dependence is opposite to that of the red wing. Increased temperature in the red wing *reduces* the probability of finding the Rb*–Xe system in the range $R \rightarrow R + dR$, which is shown in Figure 3, so from eq 4 we can conclude that $V^*(R)$ responsible for the red wing is attractive, as is shown in Figure 3. The blue wing, on the other hand, must arise from a repulsive potential. Quantitative

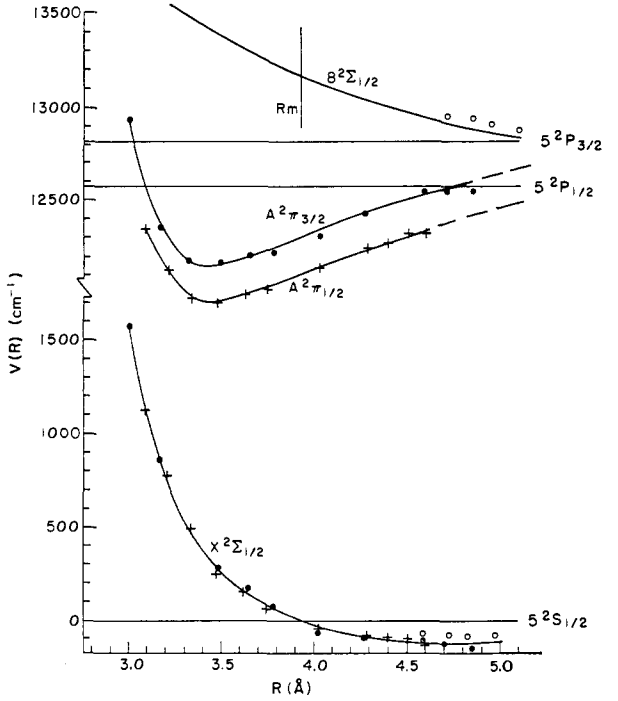

Figure 5. The Rb–Xe adiabatic potentials inferred from the data in Figure 4. (Reference 30, with permission.)

measurements of these temperature effects allow the determination of $V^*(R)$. The line shape determines $V^*(R) - V(R)$ from eq 2, and since $V^*(R)$ can be determined from the temperature dependence, the ground-state potential, $V(R)$, can then be separately determined.[30] These potentials are shown in Figure 5.

4. Collisional Redistribution

In the line-broadening experiments discussed above, the Rb atoms are resonantly excited and then the emission from the collisionally perturbed Rb* is dispersed and detected. Since measurement of $I(\nu)$ is crucial, *great* care must be taken to reject the orders-of-magnitude greater intensity due to atoms emitting at the frequency of the resonance line. To circumvent these problems, one may perform almost the reverse experiment: excite the system with light of nonresonant frequencies in the wings of the resonance line and then detect light that has been collisionally redistributed into the resonance line. One not only is thus able to exploit the single-frequency characteristics of lasers but is also able to obtain *new information* about the collision by observing the polarization of the emission relative to that of the laser.

This technique was introduced by Carlsten, Szöke, and Raymer[31] and exploited by Cooper, Burnett, and co-workers.[8,32-34] As an example of its utility, we cite the recent work of Cooper et al.[34] on the Ba–Ar and Ba–Xe systems. Line shape and depolarization measurements were made in cells containing $\approx 10^{-5}$ Torr of Ba vapor and 1–30 Torr of perturber. A CW laser of bandwidth ≈ 1 cm^{-1} was detuned ± 30–1000 cm^{-1} from the 5535-Å Ba resonance line, and the fluorescent intensity was measured as a function of polarization. Interatomic potentials were not extracted because the measurements were not made as a function of temperature, but the data served to establish qualitatively that the Π^* potential must cross the Σ^* potential, and that the Π^* potential has a deeper well. These qualitative relationships are shown in Figure 6.

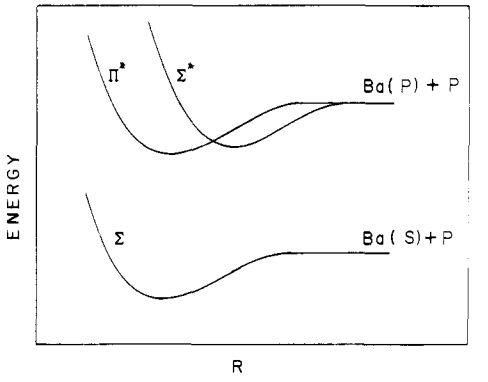

Figure 6. Qualitative sketch of the potentials inferred from collisional redistribution measurements on Ba perturbed by collisions with Ar or Xe. (Adapted from ref 34.)

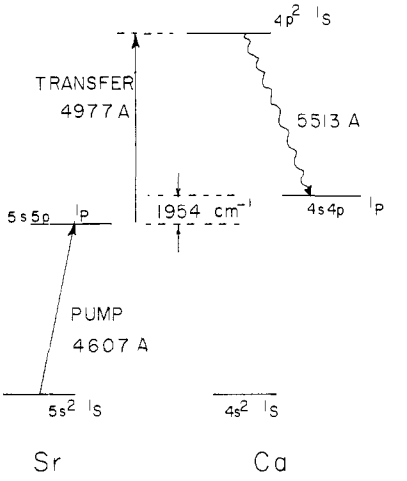

Figure 7. Energy level diagram for the Sr–Ca system. The ^{1}P level of Sr is populated by a pump laser at 4607 Å. The transfer laser at 4977 Å is absorbed *during* a collision between Sr*(^{1}P) and Ca, leading to formation of Sr(^{1}S) and Ca**(4p ^{1}S), which fluoresces at 5513 Å. Note that the transfer laser at 4977 Å is not resonant with either atom alone. (Adapted from ref 40.)

Havey and co-workers[35] recently reported fine-structure transitions in collisional redistribution of light in sodium atoms perturbed by ≈ 50 Torr of argon. The ratio of intensities found in the two D lines differs sharply for excitation in the blue or in the red for detunings of ≈ 400 cm^{-1}. The numerical results suggest that electronically nonadiabatic transitions occur after absorption, which are important in determining the distribution of atoms produced in the different states. Theoretical treatments are given in ref 36 and 37.

B. Two-Species Transitions

For these transitions, the photon is (nearly) resonant with the energy difference between an eigenstate in *one* species and an eigenstate in *another* species. The transition thus connects states in *different* atoms, with any energy defect ϵ being made up in collisional kinetic energy. These processes were first discussed by Gudzenko and Yakovlenko[38,39] and have been experimentally studied by Harris, Toshek, Bréchignac, and co-workers.[38-48]

To illustrate the physics of these processes, a schematic diagram of the "light-induced collisional energy transfer"[49] in the Sr–Ca system[40] is shown in Figure 7. The energy levels of strontium and calcium are similar,

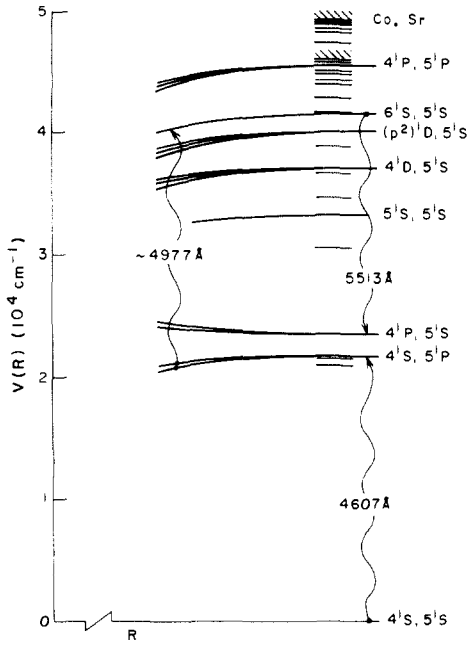

Figure 8. Quasi-molecular view of process shown in Figure 7. Ca–Sr adiabatic potentials responsible for the CaSr* → CaSr** transition near λ = 4977 Å. (Reference 52, with permission.)

but not identical, so that an excited Sr in the $^1P_1$ level cannot transfer its energy in collision to the $^1P_1$ level of Ca because it lacks 1954 cm^{-1} of energy. But if the system is irradiated at 4977 Å, sufficient energy is available to form ground-state Sr and Ca**(^1S), which can be detected by the Ca fluorescence at 5513 Å. Experimentally, Sr and Ca are contained in a heat pipe oven and Sr*($^1P_1$) is prepared by exciting Sr(^1S) with a pulsed pump laser at 4607 Å. The transfer laser at 4977 Å is delayed with respect to the pump laser to avoid direct two-photon pumping of Ca. Emission of Ca**(^1S) is observed even though *neither* isolated atom absorbs at 4977 Å. In order to observe Ca** both Sr* and Ca* are required. Emission is only observed during the transfer laser pulse, so Ca** is apparently produced in a simultaneous three-body collision between Sr*, Ca, and the laser photon. A "line shape" is obtained by tuning the transfer laser as the Ca**(^1S–$^1P_1$) fluorescence at 5513 Å is monitored, and a line ≈14 cm^{-1} wide is observed that peaks at λ = 4977 Å, corresponding to a transition between the atoms, Sr*(^1P)–Ca(^1S). The effective two-body cross section is ≈10^{-17} cm^2 at fields of ≈1 MW/cm^2 and is linear up to powers of ≈1 GW/cm^2.

Similar experiments have been carried out for transfer to other excited Ca levels,[40,41,43] and similar experiments at higher resolution have been carried out in other systems by Toschek, Brechnignac, and their collaborators.[46,48] Some experiments have begun on molecules.[47,50,51] The absorption "lines" for these energy-transfer processes represent transitions between levels in *different* atoms, and peak at the wavelength of the infinitely separated atoms, λ_∞, for dipole–dipole transitions. For multipolar transitions, the wavelength peaks near, but not at, λ_∞.[43,45]

These processes may be regarded in two ways: (1) as a radiative transition[41] by the excited atom A* and a simultaneous two-photon absorption by the colliding atom B, or (2) as formation of a complex AB‡ in collision followed by absorption to give an excited complex AB‡*, which subsequently decays to give A and B*. The quasi-molecular viewpoint,[52] shown in Figure 8 for the Sr–Ar case, describes these "two-species" events as a molecular transition in which the transition moment → 0 as $R \rightarrow \infty$. This view "demystifies" the LICET process by allowing it to be encompassed within the framework of conventional line-broadening theory and also shows that the peak absorption is not necessarily *exactly* equal to the asymptotic energy difference. This view is more useful to us, because it describes the broadening of the far wings of absorption lines, and lays a basis for treatment of multiple-species interactions, including chemical reactions.

TABLE III. Photon-Assisted Recombination

system	laser	emitter	ref
Xe/Cl_2	F_2 (158 nm)	XeCl (B, C)	53
Xe/Xe	F_2 (158 nm)	Xe_2	54
Xe/Cl_2	dye	XeCl (B, C)	15, 16, 55
Xe/Br_2	dye	XeBr (B, C)	17, 55
Mg/Mg	Ar^+	Mg_2	56
Ca/Ca	?	?	57
Sr/Sr	?	?	58
Hg/Hg	ArF (193 nm)	Hg_2	59
Xe/Cl_2	ArF	XeCl	60
Xe/Cl_2, Xe/F_2	lamp	XeCl, XeF	61

IV. Chemical Reactions (Multiple-Species Transitions)

Spectroscopic observations made on species formed during chemically reactive events are "multiple-species" transitions because the products are, by definition, different from the reagents. Some of these observations are summarized in Table I, where we have characterized the experiments according to whether the intermediate species is observed in absorption or emission. It should be mentioned at the outset that the chemical reactive systems are more complex and consequently more difficult to investigate (and to interpret!) than their related nonreactive counterparts. As a consequence, the experimenters have expended considerable effort to demonstrate that the observations do, in fact, pertain to the reaction event. We will try to convey an impression of the care lavished on these observations.

A. Absorption

1. Photon-Assisted Association

Perhaps the simplest and best documented kinds of chemical reactions that have been studied are the radiative association of atoms in excimer systems (inverse predissociation)

$$A + B + h\nu \rightarrow AB^* \qquad (5)$$

where the ground-state species, AB, is unstable. Our interest is the photoassociation process itself, but these systems are almost ideal active media for high-power molecular lasers, so photoassociation has been explored as a means of producing the excited state. Some of these systems are listed in Table III. Much attention has been devoted to the xenon–halogen systems, and we begin by considering Setser's recent work on the Xe–Br system.

(a) Xe + Br + $h\nu$ → XeBr* (B). This process is schematically shown in Figure 9. During a collision between two ground-state atoms, light can be absorbed

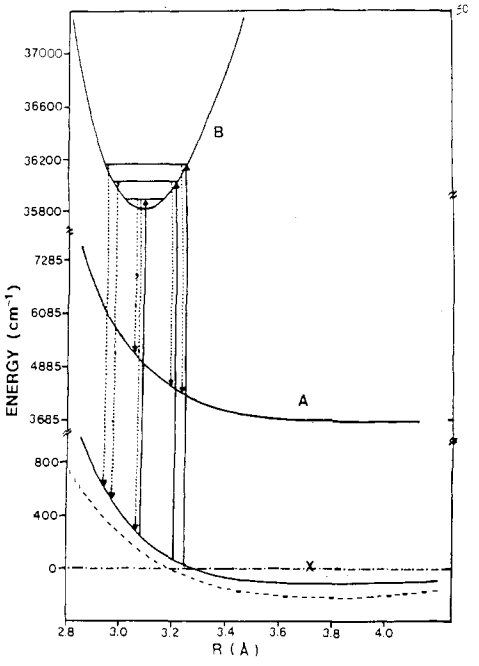

Figure 9. Potential curves for the X, A, and B states of XeBr. Photoassociation occurs as Xe and Br approach on the X state and undergo a transition to the B state as shown by the heavy vertical lines. Emissions to the A and X states are shown as dotted lines. (Reference 17, with permission.)

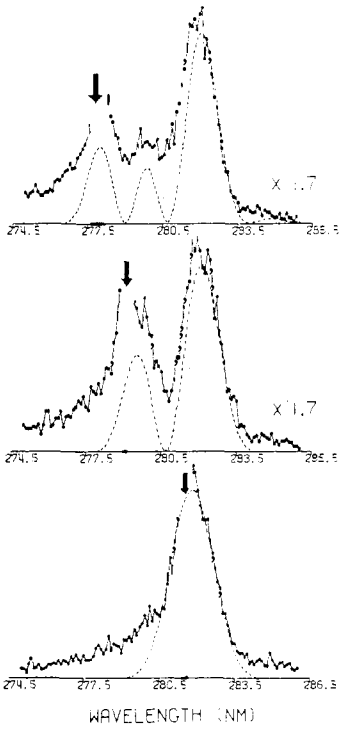

Figure 10. Fluorescence spectra for XeBr*(B, $v' = 0, 1, 2 \rightarrow X$) arising from photoexcitation of the free atoms during collision. Heavy arrows on the spectra indicate the laser wavelength for the excitation of the given XeBr* vibrational level (281.5, 279.0, and 278.0 nm for $v' = 0$, 1, and 2, respectively). Spectra are normalized for display, and the dotted curves are calculated Franck–Condon factors. (Reference 17, with permission.)

at frequencies corresponding to the energy difference between the upper and lower potential curve

$$h\nu(r) = V_u(r) - V_l(r) \quad (6)$$

where $V_u(r)$ and $V_l(r)$ are the r-dependent potential energies in the upper and lower molecular states. For XeBr, the ground-state potential is repulsive in the region where transitions are Franck–Condon allowed so only unbound species (i.e., species formed *during* a collision) can be excited.

Experiments[17,55] are carried out in 2–10 Torr of mixtures of 10% Br_2 in Xe contained in a laser fluorescence cell. A pulsed electric discharge produces Br atoms and precedes by ≈3 ms a pulse (8 ns, ≈2–15 mJ/cm^2) from a Nd:YAG pumped dye laser. Depending on the wavelength, the laser pulse selectively populates a given XeBr(B, v') level, which can be detected in fluorescence to either the A or X state. This fluorescence is dispersed with a monochromator and monitored either by fixing the monochromator and scanning the laser to provide an excitation spectrum or by fixing the laser wavelength and scanning the monochromator to provide a fluorescence spectrum.

Figure 10 shows fluorescence spectra of $XeBr_1$ (B,$v' = 0, 1, 2 \rightarrow X$) together with Franck–Condon factors calculated from the potential curves. (Similar curves are observed for the B–A emission.) The spectra clearly show "Condon diffraction patterns", which are oscillations arising from interferences between the wave function of the bound upper state and that of the continuous lower state. Similar diffraction patterns were observed earlier in the photoassociation of Hg_2[59] and Mg_2[56] and for both these molecules the Condon undulations in the spectrum were useful in determining the potential. For XeBr, the (already) known potentials for the X and B states reproduced the experiments, but the A-state potential required modification in order to fit the experiments.[17]

These spectra arise from *photoassociation* events, rather than from simple fluorescence of the reagents or from laser excitation of the reagents, followed by reaction. No Xe states are accessible in this wavelength range, and fluorescence from Br_2* states was ruled out because fluorescence was not observed from Ar/Br_2 mixtures in the wavelength range studied. Laser excitation of Br_2 followed by reaction was also ruled out because the XeBr* spectrum arising from the Xe + Br_2* reaction is quite different from that of Figure 10. The polarization of the fluorescence was also investigated,[17] and the XeBr(B) molecules were found to be preferentially formed with the plane of molecular rotation coinciding with the polarization plane of the laser.

(b) Xe + Cl + $h\nu \rightarrow$ XeCl*(B,C). The analogous Cl_2 reaction has also been studied by Setser and co-workers[15,55] with the same techniques, but the Condon diffraction pattern is less clear-cut because the van der Waals well of the ground state lies in the Franck–Condon allowed region, and bound–bound transitions from van der Waals molecules are mixed with free–bound photoassociation. The same basic features are observed, however.

McCown and Eden[16] have provided independent observation of this process at higher pressures using a laser pulse to produce Cl atoms. Two excimer lasers are focused into a cell at 300 Torr and ≈50 MW/cm^2. The first laser photolyzes the Cl_2 and the second (at various delays) is responsible for photoassociation between Xe and Cl. The XeCl* C → A emission is observed to be linear in laser fluence and Cl_2 pressure and appears *promptly* with the laser pulse. Emission from Xe_2Cl

is also observed at these high pressures.

Formation of XeCl* upon laser irradiation of Xe/Cl_2 mixtures was also reported earlier by other groups. Wilcomb and Burnham[60] reported XeCl* fluorescence after irradiation with an ArF laser, but since the ArF photon (193 nm) is *not* energetic enough to produce XeCl* + Cl, they postulated that they had observed laser-assisted photoassociation of Xe with Cl_2 to give $XeCl_2$*, which then acquired enough energy through collisions to dissociate into XeCl* and Cl. This conjecture might be supported by McCown and Eden's finding[16] that preliminary photolysis of Cl_2 with an ArF laser significantly enhances the XeCl* emission. This enhancement may be due to the XeCl* produced by photoassociation of Xe and Cl (formed in the photolysis) as well as by the mechanism of Wilcomb and Burnham (which yields XeCl* and also a Cl atom.) More experiments are needed to verify these conjectures.

Kompa and colleagues[53] reported XeCl* emission from Xe/Cl_2 mixtures on irradiation with an F_2 laser at 158 nm, and this is discussed in section IVA3e. Dubov et al.[61] made early measurements on XeF* and XeCl* produced by arc lamp irradiation of mixtures of Xe and F_2 or Cl_2.

(c) Hg + Hg + $h\nu \rightarrow Hg_2$*. Condon oscillations were observed in fluorescence from mercury vapor[59] at atomic densities ranging from 10^{17}–10^{19} atoms/cm^3, using excitation pulses from an ArF laser at 193 nm at power densities of 0.01–1 MW/cm^2. A high vibrational level of Hg_2*(O_u^+) was formed with a lifetime comparable to the time between collisions. Since thermalization does not occur (even at the higher densities), it is likely that the spectrum represents single-collision events. Many oscillations were clearly resolved, even though the combination of thermal energy in the lower repulsive state and laser bandwidth was sufficient to excite several vibrational levels of the upper state. These oscillations were independent of pressure and temperature, showing that they arise from free–bound absorption transitions to the upper state. Semiclassical simulations of the intermaxima spacing are in reasonable accord with the data, but this is insufficient to determine either potential since both potentials are unknown.

(d) Mg + Mg + $h\nu \rightarrow Mg_2$*. Scheingraber and Vidal[56] have reported extensive measurements on the discrete and continuous spectra for the Mg_2(A–X) transition. Because the van der Waals well in the X state is in the Franck–Condon region, spectra arise from excitation of both continuous and discrete levels in the X state to bound levels of the A state, followed by fluorescence again to continuous and discrete levels in the X state. Bound–bound–bound transitions result, of course, in discrete resonance fluorescence series that are in excellent agreement with calculations of discrete Franck–Condon factors. Bound–bound–free transitions give fluorescence that displays Condon type oscillations on an underlying continuum. The oscillations can be completely characterized by discrete excitation to the A state followed by fluorescence to the unbound X state, and the repulsive portion of the X state was determined up to 3400 cm^{-1} above the dissociation limit of the X state.

The underlying continuum (free–bound–free [FBF] transitions) arises because the nonselective excitation from the distribution of free collision pairs populates many bound levels in the A state. Fluorescence from each of these presumably results in a structured continuum with slightly different maxima, so the superposition of many such spectra would tend to smear out any oscillations and yield only an unstructured continuum. (Free–bound–bound transitions yield a discrete, but complex, spectrum which arises from the superposition of many discrete spectra.) Note that *structured* FBF fluorescence was observed in Hg_2, XeCl, and XeBr, so the superposition of many spectra arising from a continuum state frequently retains some structure. Tellinghuisen has extensively discussed the application of the Franck–Condon principle to bound–free transitions.[62]

TABLE IV. Photon-Assisted Ionization

system	laser	detected	ref
Na/Na	vis	Na_2^+, Na^+	63, 64, 65
Na/Li	vis	$NaLi^+$	14b
Li/Li	vis	Li_2^+, Li^+	66
Ba*/Na	vis	Na^+	14a
He*/He	355 nm	ions	67

2. Photon-Assisted Associative Ionization

Laser-assisted associative ionization

$$A + B + h\nu \rightarrow AB^+ + e^- \quad (7)$$

is a simple process that is extremely attractive for study from an experimental point of view, because *all* of the ions can be collected and counted with high efficiency. But ionization energies are typically high enough that either VUV photons or electronically excited reagents are required, and this complicates experiments. Photon-assisted associative ionization has been observed in a few systems, and these are listed in Table IV.

(a) Alkali Metal–Alkali Metal Association. Weiner and co-workers have extensively studied several ionization processes in alkali metals

$$M^* + M' + h\nu \rightarrow MM'^+ + e^-$$

photon-assisted associative ionization

$$M^* + M' + h\nu \rightarrow M^+ + M' + e^-$$

photon-assisted Penning ionization

and

$$M^* + M'^* \rightarrow MM'^+ + e^-$$

(normal) associative ionization

where M and M′ denote alkali metals, and M* denotes (usually) the first excited p state. These experiments have been conducted in *crossed atomic beams*, so while many possible interfering collisional processes are avoided, the signal levels are generally low, and much of the work has been devoted to establishing the observation of the laser-assisted process.

In the first system to be studied,[66] two Li atom beams were crossed in the field of two flash-pumped dye lasers of intensity <0.1 MW/cm^2, and Li^+ and Li_2^+ ions were detected with a mass spectrometer. If laser 2 was tuned to the 2s–2p transition in Li at 6707 Å, the ion intensity was observed at several different laser 1 wavelengths and was linear in laser 1 intensity. But both atomic beams were required and laser 2 had to be tuned to the Li atom resonance. Formation of Li_2^+ from two Li(2p) atoms is endoergic by 0.74 eV, and since laser 1 was not

resonant with any Li atom transitions, the authors concluded that the laser-assisted process

$$Li^* + Li^* + h\nu \rightarrow Li_2^+ + e^- \quad (8)$$

had been observed. Ionization processes originating from Li dimers were discounted by the authors because the signal depended linearly on the laser power.

Somewhat similar experiments were reported[14b] with beams of Na and Li crossed in the field (50 kW/cm^2) of just one laser. The $NaLi^+$ ion was observed only when the laser was tuned to the Na 3s–3p transition and was linear in laser intensity. Associative ionization of Li + Na* is highly endoergic, so it was postulated that the process

$$Na^* + Li + h\nu \rightarrow NaLi^+ + e^- \quad (9)$$

had been observed, which was linear in laser intensity since the Na transition was saturated.

The Na/Na system was studied, again in crossed beams, in a two-laser field, where one (weak) laser was set to the Na 3s–3p transition and the second (≈30 MW/cm^2) was scanned.[63] Photon-assisted associative ionization was again observed, and structure was observed in the excitation spectrum (ion signal vs laser wavelength). But as testimony to the difficulty of these experiments, subsequent work on this system[64,65] has shown that the structure is likely due to multiphoton processes in trace amounts of Na_2 present in the beams. The structure rides on a continuum that arises from a process of atomic origin, which is thought to be the laser-assisted reaction.

(b) He* + He + *h*ν. Pradel et al.[67] have observed He^+ ions resulting from single collisions between He*-(2^1S,2^3S) and He in the presence of a laser field ≈10 MW/cm^2 at $h\nu$ = 3.49 eV (λ = 355 nm). A beam of fast He* atoms traversed a scattering cell at E_{cm} = 35 or 50 eV, and He^+ ions were detected at zero scattering angle. Penning ionization is energetically possible from both a diabatic nonresonant process

$$He^* + He \rightarrow He^+ + He + e^- \quad (10)$$

and a photon-assisted process

$$He^* + He + h\nu \rightarrow He^+ + He + e^- \quad (11)$$

A time-of-flight analysis (acquired over a counting period of 17 h!) showed that He^+ ions produced from the photon-assisted process (11), which occurred only when the laser pulse was present, could be distinguished from those produced by the purely collisional process (10). Comparison of signals from both processes allowed the cross section for (11) to be estimated as $\sigma_a \approx 4 \times 10^{-18}$ cm^2 in a field ≈10 MW/cm^2.

The laser-assisted channel (11) is the only process consistent with the following observations: both He* and $h\nu$ were required, and the laser was not resonant with any atomic transitions. No molecular contaminants were expected, and σ_a decreased with increasing collision energy, which is opposite in direction to σ_d for the diabatic process (10).

3. Photon-Assisted Bimolecular Reactions

The simplest bimolecular reaction is the atom exchange reaction

$$A + BC \rightarrow AB + C \quad (12)$$

TABLE V. Photon-Assisted Bimolecular Reactions

system	laser	power, MW/cm^2	detected	ref
K + $HgBr_2$	green	2	HgBr*	9
K + NaCl	red	0.002	Na*	10, 11
Mg + H_2	UV	1	LIF of MgH	13
Xe + Cl_2	2 UV	400	XeCl*	55, 68
	VUV	≫2		54

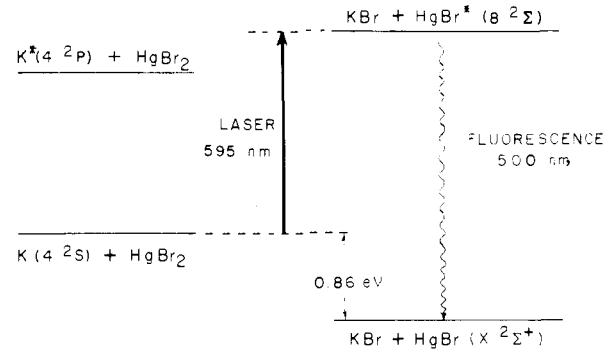

Figure 11. Energy level diagram for the reaction K + $HgBr_2$ → KBr + HgBr, which was studied in crossed molecular beams. Emission of HgBr* at 500 nm was observed in the presence of a laser tuned to the blue of 606 nm, even though neither reagents nor products absorb in this wavelength range. It was concluded that the photon was absorbed during the chemically reactive collision. (Reference 9.)

At some time in the course of these reactions *new* species, [A···B···C], must appear which are *neither* reagents *nor* products, which we will call transition region species and which might be expected to absorb light at wavelengths different from either reagent or product. Virtually all chemical reactions should exhibit this behavior, so we expect that, in general, light can be absorbed in the course of reaction. But the lifetime of the transition region species is expected to be so short that, in general, light absorption during reaction will constitute a vanishingly small perturbation of the observables. The problem facing the experimentalist then is to design a system where the effect of photon absorption during collision can be observed and separated from other, more mundane, effects. The systems studied so far are collected in Table V.

(a) K + $HgBr_2$ + *h*ν → KBr + HgBr*. In order to *detect* photon-assisted reaction a reaction was sought where a photon, which was not resonant with either reagents or products, could open a new reaction channel to an excited product

$$A + BC + h\nu \rightarrow AB + C^* \quad (13)$$

which could then be detected in fluorescence

$$C^* \rightarrow C + h\nu' \quad (14)$$

If the reaction were exoergic, the fluorescent photon could be blue shifted compared to the exciting photon, so $\nu' > \nu$. These criteria were satisfied by the reaction

$$K + HgBr_2 + h\nu \rightarrow KBr + HgBr^* \quad (15)$$

The dark reaction is ≈20 kcal/mol exoergic, so photons with wavelength shorter than ≈606 nm are sufficiently energetic that absorption of such a photon by a transition region species [$KHgBr_2$] could produce HgBr*-($B^2\Sigma$) which fluoresces to the X state at 500 nm. The energetics are illustrated schematically in Figure 11.

Because the dark reaction

$$K + HgBr_2 \rightarrow KBr + HgBr \quad (16)$$

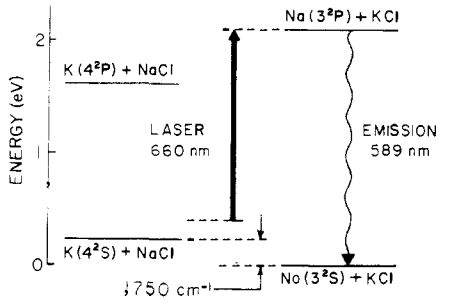

Figure 12. Energy level diagram for the reaction K + NaCl → KCl + Na, which was studied in crossed molecular beams. The energy required for formation of Na* is provided by the photon, by the thermal energy (shown as a dotted region), and by the reaction exoergicity. Emission of Na* is used to monitor the absorption. (Reference 10.)

occurs on nearly every gas-phase collision,[69] measurements in the gas phase under static conditions were not possible. The reaction was consequently studied by crossing molecular beams of K and $HgBr_2$ in the cavity of a flash-pumped dye laser (FPDL) tuned to $\lambda = 595$ and 600 nm and monitoring the (B → X) fluorescence at $\lambda = 500$ nm. As shown in Figure 11, at these wavelengths no single-photon absorptions are possible in either the reagents or the products. A small amount of extra fluorescence was observed when all three beams were on. Auxiliary experiments with a Nd:YAG pumped dye laser (narrower bandwidth and shorter pulse) suggested that this was not a multiphoton effect, that the fluorescence was prompt, and that the emitter had a lifetime comparable to that of $HgBr^*(B^2\Sigma)$. We concluded that we had observed the photon-assisted reaction, and from the magnitude of signal and beam intensities, roughly estimated the cross section, $\sigma_c \approx 0.1$ Å^2 in a laser field of ≈ 2 MW/cm^2.

Even though the cross section is not too small, it is still only $\approx 10^{-3}$ of the dark reaction, and moreover the photon-assisted reaction only occurs *during* the very short time (≈ 1 μs) of the laser pulse. Signal counts were ≈0.1 per laser shot, and extensive averaging was required to obtain $S/N \approx 5$–10. Since the average number of signal counts is expected to be proportional to the average laser power (≈0.6 W for the FPDL), the apparatus was modified to lie within the cavity of a CW dye laser where the average circulating power was ≈100 W. After some initial difficulties because of new interferences arising from multiphoton processes in K_2, signals with $S/N \approx 10$ were obtained at several excitation wavelengths.[70] These signals require the presence of all three beams, and support our earlier conclusion that we had observed the photon-assisted reaction. Unfortunately, the expected large increase in signal intensity was not obtained, and because of the corrosive and poisonous nature of $HgBr_2$ we have discontinued experiments on this system.

(b) K + NaCl + $h\nu$ → KCl + Na*. Because of the difficulties associated with the $HgBr_2$ system, our laboratory[10,11,70] has more extensively studied the K–NaCl system shown schematically in Figure 12. The dark reaction

$$K + NaCl \rightarrow KCl + Na \qquad (17)$$

is once again exoergic and proceeds on roughly every gas-phase collision,[71] so the reaction is again studied in crossed molecular beams. Because of the exoergicity,

TABLE VI. Count Rates (±1σ) for Observation of Na D Radiation with Various Combinations of K, NaCl, and Light Beams for Irradiation at λ = 670 nm

signal	origin (elementary process)	count rate, s^{-1}
R_{000}	dark current	2.4 ± 1
R_{001}	scattered light	30.2 ± 2
R_{100}	K background	2.7 ± 1
R_{010}	NaCl background	7.0 ± 1
R_{101}	K photoluminescence	169.7 ± 6
R_{011}	NaCl photoluminescece	44.6 ± 4
R_{110}	chemiluminescence	7.0 ± 2
R_{111}	three-beam signal	481.5 ± 12

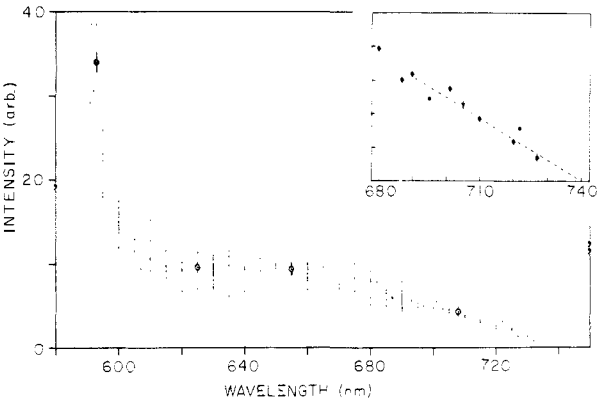

Figure 13. Excitation spectrum for the reaction K + NaCl + $h\nu$ → KCl + Na*. Emission of Na*(3p ^{1}P) at 589 nm is used to monitor the reaction as the wavelength of the exciting laser is varied. The inset shows the behavior observed at the experimentally determined threshold. The spread in points is indicative of the reproducibility of the signal, and no structure is discernible at this S/N level. The experimental threshold is consistent with a thermodynamic upper wavelength limit of 924 nm. A more accurate theoretical threshold requires accurate bond dissociation energies and a knowledge of how much initial energy is available for reaction. (Reference 10.)

photons to the red of the Na D line are able to excite the [NaKCl] system to an energy state from which Na* and KCl can evolve. The threshold for this process depends on how much rotational, vibrational, and translational energy is available, and how much can be converted into Na*. Once again, no single-photon absorptions occur in the reagents or products in the wavelength range that was used.

Molecular beams of the reagents were crossed inside the cavity of a CW dye laser, and fluorescence from Na* was viewed through an interference filter and monitored by a cooled photomultiplier tube. The circulating power in the cavity was ≈100 W (unfocused), resulting in a power density ≈1.5 kW/cm^2. The laser bandwidth was ≈1.5 cm^{-1}, and the band-pass of the interference filter was ≈0.5 nm. Data were taken in all eight beam on–beam off combinations, and contributions from various elementary processes to the signal were deconvoluted, leading to an analysis such as that shown for illustration in Table VI. (Each *actual* count rate is a sum of one or more elementary processes; see ref 10 and 70 for details of this analysis.) The signal of interest in Table VI is the 3-beam signal, which is the signal when all three beams are on, corrected for various other (0-, 1-, and 2-beam contributions to the signal.

Table VI and similar data at other wavelengths demonstrate that the 3-beam signal is statistically highly significant. These signals extend over a very large range of laser wavelengths, and an excitation spectrum (Na* fluorescence vs laser wavelength) is

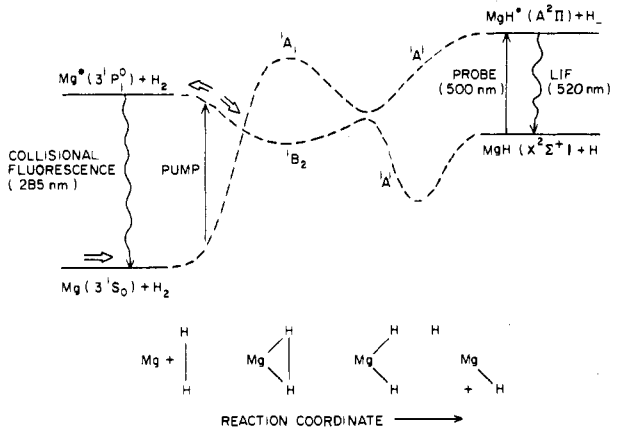

Figure 14. Energy levels for the reaction Mg + H_2 + $h\nu$ → MgH + H (schematic). The pump laser (shown here in the red wing of the Mg resonance line) excites a MgHH transition region species which can evolve either reactively to form MgH, detected by laser-induced fluorescence, or nonreactively to form Mg*, which is detected in fluorescence. (Reference 13, with permission.)

shown in Figure 13. The spectrum is rather featureless and the threshold near 735 nm is consistent with the known thermochemistry. The 3-beam signal is measured to be linear in the flux of each of the three reagents: K, NaCl, and photons. Multiphoton processes are consequently ruled out.

Extensive tests have been made to determine if excitation of trace quantities of K_2, followed by some collisional deexcitation, could account for the signal. In the most conclusive test,[11] the K beam was passed through an inhomogeneous magnetic field that discriminated against K_2 molecules. The signal was observed to depend on the paramagnetic species present in the beam (presumably K atoms), so processes involving K_2 are *not* involved.

We believe that these experiments can be most easily interpreted as observation of the laser-assisted reaction

$$K + NaCl + h\nu \rightarrow KCl + Na^* \quad (18)$$

We view this process as the formation and subsequent excitation of a transition region species, [KNaCl]

$$K + NaCl \rightarrow [KNaCl] \quad (19)$$

$$[KNaCl] + h\nu \rightarrow [KNaCl]^* \quad (20)$$

followed by decomposition of the excited transition region species to products, which in turn fluoresce:

$$[KNaCl]^* \rightarrow KCl + Na^* \quad (21)$$

$$Na^* \rightarrow Na + h\nu' \quad (22)$$

Nonreactive decomposition to K* and NaCl is likely on energetic grounds, and copious signals have been observed at the K D lines. These signals may arise from other sources, and we have not yet performed experiments necessary to identify their origin.

(c) Mg + H_2 + $h\nu$ → MgH + H. The reaction between magnesium vapor and hydrogen is highly *endoergic* so Kleiber et al.[13] have studied this laser-assisted reaction in the gas phase, rather than in crossed beams. MgH is formed only in laser-assisted collisions, and is detected by fluorescence induced by a second laser.

An energy level diagram for this system is shown in Figure 14. A Nd:YAG pumped dye laser is tuned near the Mg($3\,^1P$–$3\,^1S$) transition at 285 nm and softly focused into a hot (700 K) oven containing ≈ 0.5 mTorr of Mg and ≈4 Torr of H_2. The laser power density is estimated to be ≈1 MW/cm². Transition region species are expected to form and to absorb this light

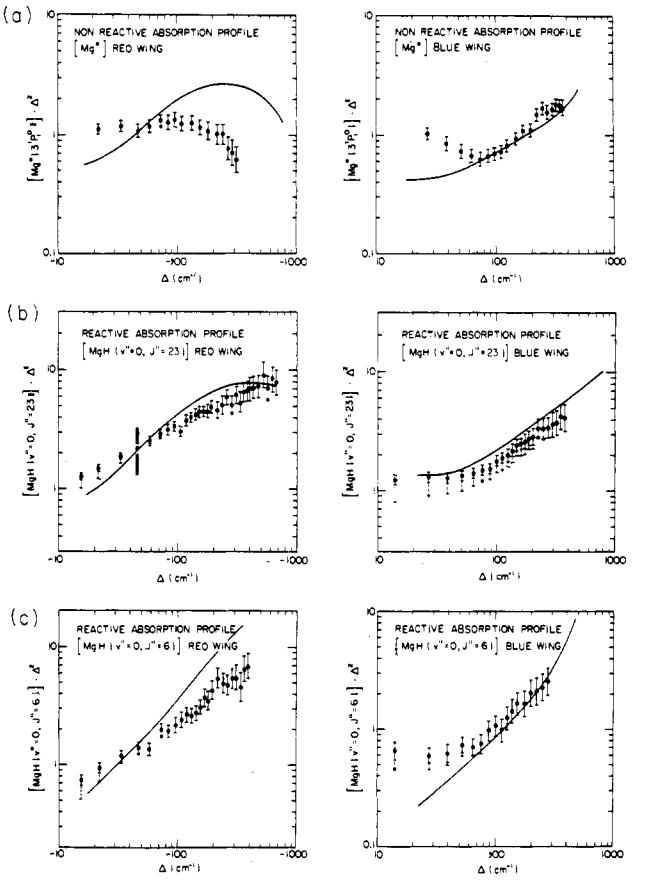

Figure 15. Experimental far-wing laser absorption profiles for the Mg + H_2 reactive collision system: (a) nonreactive signal (emission of Mg*); (b) reactive signal (laser-induced fluorescence) from the $v'' = 0$, $J'' = 23$ level of MgH as a function of laser detuning [$\Delta \equiv \omega_L - \omega_0$]. The profiles have been multiplied by the factor Δ^2, which is found to accentuate some spectral features found in some nonreactive systems. Solid curves are model theoretical predictions. (Reference 13, with permission.)

$$Mg + H_2 \rightarrow [MgH_2] \quad (23)$$

$$[MgH_2] + h\nu \rightarrow [MgH_2]^* \quad (24)$$

and are likely to decompose to either excited reagents

$$[MgH_2]^* \rightarrow Mg^* + H_2 \quad (25)$$

or products MgH + H

$$[MgH_2]^* \rightarrow MgH + H \quad (26)$$

Nonreactive decomposition of the excited transition region species, reaction 25, is detected by the emission of atomic Mg at 285 nm. The chemically reactive channel (26) is probed by a second pulsed dye laser tuned to the MgH($A^2\Pi$–$X^2\Sigma$) transition. The probe laser pulse is delayed 7 ns to avoid two-photon processes. This delay is believed to be short enough to minimize observation of secondary collision processes leading to the formation of MgH or observation of the rotational relaxation of the nascent MgH product.

Typical laser absorption profiles are shown in Figure 15. Both reactive and nonreactive signals are observed over a range of hundreds of wavenumbers on either side

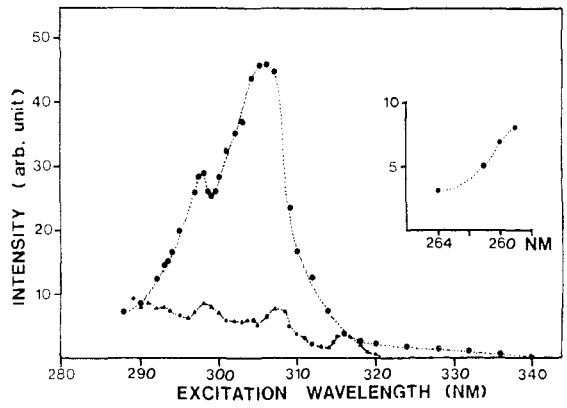

Figure 16. Excitation spectra for the reaction Xe + Cl_2 + $2h\nu$ → XeCl* + Cl. The emission of XeCl(B–X) was monitored at 308 nm. Reaction to form XeCl* was also observed for mixtures of Xe with ICl and CCl_4. (Reference 55, with permission.)

of the Mg resonance line. These signals are linear in pump laser power, H_2 pressure, and Mg density. Various artifact sources of signal such as amplified spontaneous emission from the laser, multiphoton processes, absorption of Mg_2, and so on have been discounted. The largest artifact source is believed to be the resonant excitation of Mg and subsequent reaction of Mg*, and this is discounted on the basis of Breckenridge and Umemoto's direct study of the Mg* + H_2 reaction.[72] Processes 23–26, formation and excitation of a transition region species, thus offer the most reasonable explanation of the experimental data.

Interpretation of their results is discussed in section VI.

(d) Xe + Cl_2 + $nh\nu$ → XeCl* + Cl. Several groups have reported studies of xenon halide emission following irradiation of mixtures of xenon and halogens.[17,53,55,60,61] The most detailed of these have been reported by Setser et al.[17,55] They irradiated 10–20% mixtures of Xe/Cl_2 and Xe/ICl at pressures of 3–15 Torr with pulses from a YAG–DYE–SHG laser at wavelengths in the range 290–316 nm and power densities ≈400 MW/cm^2. Emission from the XeCl or XeI excimers in the B–X bands near 308 nm was easily observed. This emission was determined to be quadratic in laser intensity, linear in Xe pressure, and linear for low Cl_2 pressures. The fluorescence–time profile is an important diagnostic, but the decay kinetics are complicated. Nevertheless, XeCl* is formed during the laser pulse, showing that this is a direct, laser-assisted process. The excitation spectrum is very broad and is shown in Figure 16.

Reaction to form XeCl* is endoergic unless at least *two* photons are absorbed. The XeCl* fluorescence intensity is dependent on the square of the laser power, indicating that this is a two-photon process. Direct excitation of Xe or Cl_2 is discounted, and the fluorescence from the single-photon photoassociation process discussed in section IV.A1.b not only is negligibly weak compared to the two-photon process but also leads to a different excitation spectrum. The most likely source of XeCl* is thought to be the two-photon excitation from the unbound Xe–Cl_2 potential surface to the reactive potential surface

$$Xe + Cl_2 + 2h\nu \rightarrow [XeCl_2]^* \rightarrow XeCl^* + Cl \quad (27)$$

Kompa and colleagues[53] also reported emission from the B and C states of XeCl following irradiation of Xe/Cl_2 mixtures ($P \approx 200$ Torr) with an F_2 laser (158 nm) at powers >1 MW. (The irradiated area is not specified.) The fluorescence in these experiments was observed to depend linearly on the laser power, as well as on the Xe and Cl_2 pressure. The fluorescence again was observed to occur during the laser pulse as expected for a laser-assisted process. Since this wavelength is just half of that used in the experiments of Setser et al., it seems possible that transitions between the same surfaces are being explored. In these experiments, much of the laser pulse was *absorbed* (≈85% at 200 Torr) so an alternative explanation of the observations is that the system is bound as a van der Waals molecule in the lower state. (See also section V.)

(e) Hg* + $HgBr_2$ + $h\nu$ → HgBr* + HgBr. Hg*(6 $^3P_1$) has an ionization potential of 5.5 eV so the reaction surface for Hg* + $HgBr_2$ was thought to be similar to that for K + $HgBr_2$. The ground-state reaction

$$Hg + HgBr_2 \rightarrow 2HgBr \quad (28)$$

is endoergic by 2.34 eV so it was possible to study this system in the gas phase.[12] A Nd:YAG pumped dye laser was frequency doubled and Raman shifted to the 2537-Å resonance (6 $^3P_1$–6 $^1S_0$) of Hg. The UV laser pulse (100 μJ and 6 ns) and part of the infrared YAG pulse (1.06 μm, >100 mJ, 9 ns) were focused into a gas cell containing ≈10^{15} molecules/cm^3 of Hg and of $HgBr_2$ with 58 Torr of He as a buffer gas. Fluorescence of HgBr* was observed by a PMT through a filter at 500 nm. A large number of experimental parameters were varied.

Fluorescence appeared to arise from the B state of HgBr, vary linearly with IR laser power, and vary linearly with UV laser power. Both reagents were necessary. The temporal dependence of the fluorescence gave a decay comparable to the lifetime of HgBr* and showed that maximum signal occurred when the IR and UV pulses overlapped temporally.

While it is tempting to interpret these observations in terms of the IR absorption of a transition region species [Hg*$HgBr_2$], it should be noted that the measurements were made in the presence of a considerable multiphoton background. This background was not linear in laser intensity, and was subtracted out. Nevertheless, caution must be exercised. One troubling aspect of an interpretation regarding the excitation of [Hg*$HgBr_2$] is that the UV power should have been more than enough to saturate the Hg(6 $^3P_1$–6 $^1S_0$) transition, so a multiphoton process with the first step saturated may provide an alternate interpretation.

(f) van der Waals Molecules. Photon absorption by van der Waals molecules in equilibrium with reagents may be responsible for some of the *gas-phase* phenomena described so far, rather than photon absorption by transition region species. Absorption by a van der Waals molecule is a qualitatively different process from the absorption by a transition region species, and is discussed in section V. We mention here experiments that specifically probe chemical reactions via these van der Waals molecules.

In several cases, van der Waals molecules have been deliberately produced in a high-pressure free jet[73–76] and then irradiated with the doubled output from a Nd:YAG pumped dye laser. The {Hg···Cl_2} system was irradiated near 250 nm and the fluorescence of HgCl* was monitored at 500 nm.[75] The {Hg···H_2} system[76] was

excited near the $Hg(6\ ^1S_0–6\ ^3P_1)$ transition at 253.7 nm, after which the $\{Hg\cdots H_2^*\}$ species then had enough energy to fragment into HgH + H or into several different states of the Hg atom. These different channels were detected by laser-induced fluorescence as the wavelength of the pump laser was swept. In contrast to *nonreactive* systems[74] such as Hg···Ne, fluorescence of the bound van der Waals complex is not observed, so nonradiative processes, presumably chemically reactive decomposition, occur at a faster rate than the fluorescence of the complex. The complex may decay to yield the $^3P_0$ state of Hg, but this is observed to be 3 orders of magnitude less efficient than decomposition to HgH. The rotational state distribution of the HgH produced was observed to be different depending on whether the complex was irradiated $\approx$25 cm^{-1} to the blue or to the red of the $Hg(^1S_0–^3P_1)$ free atom transition, corresponding to excitation of the Σ or Π states in the Hg···Ne complex. These distributions are different still from the HgH rotational distribution that results from reaction of Hg* with H_2. This shows that the experimental observations result from decomposition of the excited van der Waals complex.

A wealth of information about the $\{Hg\cdots H_2\}$ system was obtained from the experimental data, which consisted of (1) measurements of total fluorescence vs UV wavelength (fluorescence excitation spectra), (2) fluorescence of a specific quantum state vs UV wavelength (action spectra), and (3) fluorescence measurements as the probe laser is scanned at fixed UV wavelength (product spectra). Interpretation of these data suggests that reaction to form HgH from the Π state is direct ($\approx$0.1 ps) since the action spectrum is continuous, whereas reaction from the Σ state is indirect since rovibrational structure is observed. Other inferences are also drawn, such as those regarding the angular dependence of the exit channel, and suggest that van der Waals spectra may be quite informative regarding reaction dynamics.[76]

Boivineau, LeCalvé, Castex, and Jouvet have also reported[73] the observation of XeBr* and XeCl* formed in two-photon excitation of $\{Xe\cdots Br_2\}$ or $\{Xe\cdots Cl_2\}$.

B. Emission

1. Activation by Chemical Reaction

(a) $F + Na_2 \rightarrow [NaNaF]^{\ddagger *}$. The reaction of fluorine atoms with sodium dimers

$$F + Na_2 \rightarrow [NaNaF]^{\ddagger *} \rightarrow Na^* + NaF \qquad (29)$$

is exoergic by 4.5 eV and $Na^*(3\ ^2P)$ is formed as a chemiluminescent product. Polanyi and his collaborators[3,18] have dispersed the emission emanating from the intersection of crossed, uncollimated beams of F and Na_2, and find not only copious emission at the D lines but also weak emission several hundred angstroms from the D line. They interpret this as evidence of emission from an excited transition region species, $[NaNaF]^{\ddagger *}$.

The lifetime of Na* is $\approx$10 ns and that of $[NaNaF]^{\ddagger *}$ is $\approx$1 ps, so about 1 in 10^4 Na* will emit while they are in the close vicinity of the nascent NaF, or equivalently, about 10^{-4} of the D line intensity will be emitted by a transition region species, $[NaNaF]^{\ddagger *}$. These qualitative notions are substantiated by the experiments, as shown in the emission spectrum in Figure 17. The "wing"

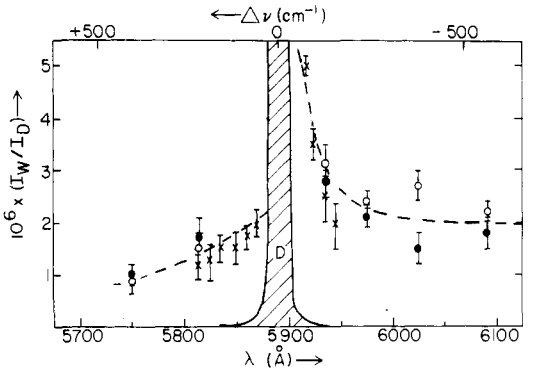

Figure 17. Emission spectrum from the very exoergic dark reaction $F + Na_2 \rightarrow NaF + Na^*$ studied in crossed jets. Most emission occurs at the Na D line, but some Na* emit *during* the collision and contribute to the intensity in the wings. Dashed curves are estimates of the wing profiles. (Reference 18, with permission.)

spectrum has been distributed over $\approx$100 elements, so the intensity in a given element is expected to be $\approx 10^{-6}$ of the D line intensity, which is observed. Note that excitation is due to chemical reaction; *no laser is involved.*

The spectrum is not sufficiently colorful to unambiguously assign it to $[NaNaF]^{\ddagger *}$, so extensive cross-checks were necessary to eliminate various artifact contributions:

(1) The reaction occurred in crossed beams, so the pressure was too low to broaden the D line in secondary collisions that might have occurred after the primary collision in which Na* was formed.

(2) Reaction 29 was determined to be the main source of emission at the D line, so the D line emission was used to monitor the product of concentrations, $[F][Na_2]$.

(3) The intensity and shape of the wings were similar to that expected. (One expects the intensity to decrease upon moving away from the D line, because emission close to the D line arises from almost unperturbed configurations in which the Na* is far from the NaF.)

(4) Other sources of emission were excluded, including Na_2^*, NaF*, and impurities in the atomic fluorine discharge.

(5) Wall reactions could be ruled out because no sodium-coated surfaces were visible to the spectrometer.

These observations are discussed in detail in the paper of Arrowsmith et al.[18b] It is reasonable to conclude from these observations that the wing emission is due to a transition region species, $[NaNaF]^{\ddagger *}$.

On the basis of some collinear potentials calculated for similar systems, these authors speculate that the red wing and the blue wing may arise from different excited-state potential curves. Even though this possibility is very appealing, they also found that the red and blue wings could be reasonably well interpreted as characteristic of the reaction pathway on the lower surface. The experimental data are presently insufficient to be able to distinguish between these models of the transition region spectrum.

2. Activation by Photodissociation

(a) $O_3^* \rightarrow O_2 + O + h\nu$. The absorption spectrum of O_3 in the Hartley bands (300–220 nm) is a continuum corresponding to excitation of a *repulsive* state that photodissociates on a time scale of a few *femtoseconds.*

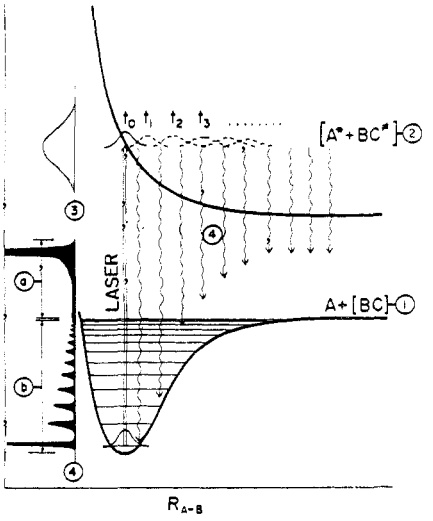

Figure 18. Schematic description of a photodissociation/fluorescence experiment. Laser excitation transfers the ground-state wave packet to the repulsive excited state where it evolves into photoproducts A + BC (as shown by wave packets at t_1, t_2, etc.). The absorption spectrum 3 is broad and featureless, but even though the dominant process is *photodissociation*, the wave packet can *fluoresce* to either the bound lower state or the continuum as denoted in (4a) or (4b). The dissociating molecule will emit at frequencies characteristic of the *ground* state, but the intensities will be governed by the dynamical behavior on the *upper* state. (Reference 4, with permission.)

Excitation of O_3 in these bands thus efficiently fragments the molecule:

$$O_3 + h\nu \rightarrow [O_3]^* \rightarrow O_2^*(^1\Delta_g) + O^*(^1D) \quad (30)$$

Both of the products are metastable, so neither one emits. It is possible, however, for a small fraction of O_3^* to emit *during* the dissociation.[4,19] For example, if the lifetime for emission is ≈10 ns and the lifetime for dissociation is ≈1 fs, about 10^{-7} of the excited O_3 will emit light rather than dissociate. This emission represents a transition from a *well-defined* energy state (which is evolving in time) in the continuum to various bound levels of the ground state as shown in Figure 18. This process resembles a Raman spectrum and is also known as "continuum resonance Raman scattering", but, as Kinsey and co-workers suggest,[4] is better described as "the emission of a molecule in the process of falling apart".

As shown in Figure 18, the exciting laser transfers probability density from the $v = 0$ level of the ground state to the upper state. The wave packet then evolves in time on the upper state by spreading out and moving to larger internuclear distance. This evolution of the wave packet on the upper surface is the photodissociation process. The wavelengths that are emitted are Raman shifted with respect to the exciting light by amounts that are characteristic of the ground state, but the *intensities* of these various transitions depend on how the wave packet evolves on the upper surface. The intensities of these emissions are thus characteristic of the dynamics in the upper state. Note that since one starts with a stable species, optical excitation to the photodissociating state leads to a state with a known amount of energy and angular momentum. This is in sharp contrast to the systems formed during collision where no amount of experimental refinement or state selection can eliminate the distribution over impact parameter. (Heller and co-workers[77] have shown that this time dependence can be Fourier transformed into a frequency dependence.)

Kinsey and his colleagues[4,19] have carefully dispersed the radiation from low-pressure (1–2 Torr) samples of O_3 irradiated with the fourth harmonic of a Nd:YAG laser at 266 nm. The spectrum is shown in Figure 19, and consists of overtones and combination bands of the symmetric stretch and even-numbered levels of the asymmetric stretch. Bending vibrations are conspicuous by their absence, and one can conclude that the change in bond angle upon excitation is slight and that the curvature of the surface with respect to the bending coordinate is similar in the upper and lower states.

The symmetry of O_3 complicates the dynamics because the initial equivalence of the O–O bonds requires that the wave packet evolve by spreading, rather than by simple motion of the center of the packet. Nevertheless, a reasonably simple picture has emerged from the experimental observations and from ab initio calculations.[78] As shown in Figure 20, the upper potential

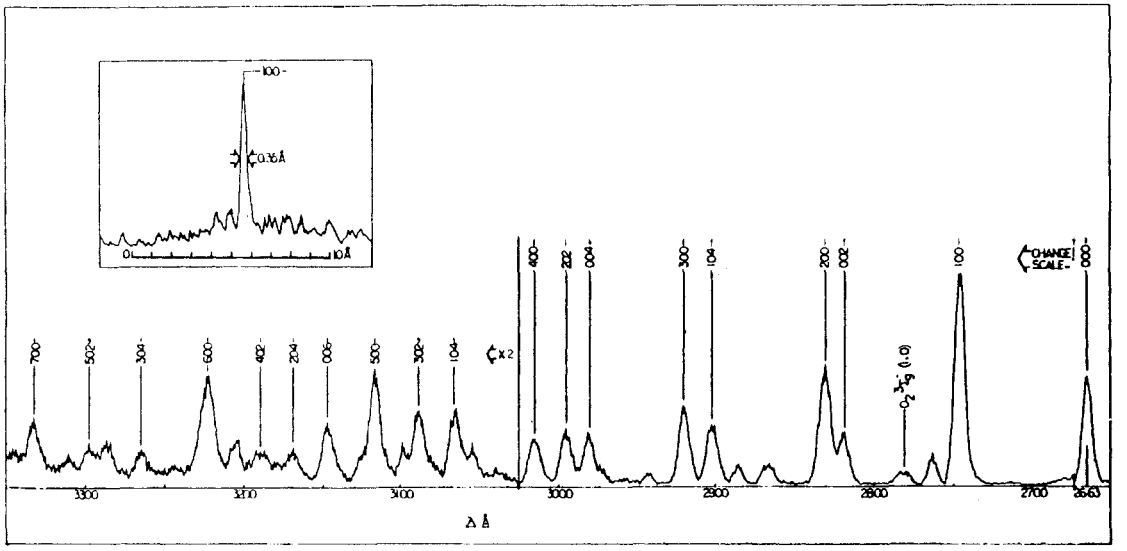

Figure 19. Emission spectrum of ozone excited at 266 nm. The spectrum consists of overtones and combination bands in ν_1 (symmetric stretch) and even quanta of ν_3 (asymmetric stretch). No bands with $\nu_2 \neq 0$ are apparent. Inset shows a high-resolution scan of the (100) band. (Reference 4, with permission.)

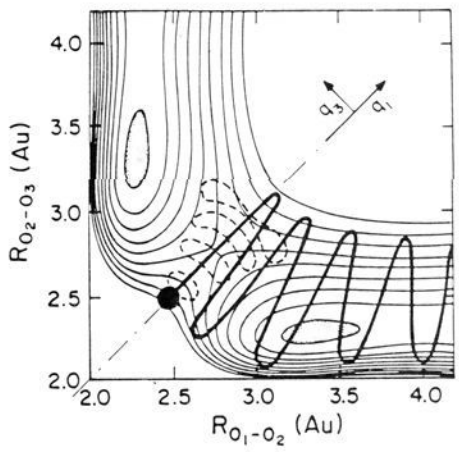

Figure 20. The ozone B_2 excited-state surface along the two stretch coordinates (q_1 and q_2), with the bending coordinate fixed at the ground-state value. The photoexcitation process produces O_3* high on the repulsive wall of the B state, and is shown as a heavy dot. A photodissociation trajectory is shown in heavy line, and the spreading wave packet is shown in dashed lines. The gray areas indicate the quasi-bound regions in the exit channels. (Reference 4, with permission.)

surface has a maximum near the ground-state nuclear configuration, so laser excitation transfers ground-state probability density to a point near the top of a saddle point on the upper surface. The wave packet evolves by spreading in a symmetrical stretching of the molecule so there is no overlap with the antisymmetric odd vibrational quanta of the lower state, and only even quanta are observed in the asymmetric stretch. Eventually the spreading bifurcates and the wave packet proceeds to products, as suggested by the trajectory of Figure 20.

(b) $CH_3I^* \rightarrow CH_3 + I + h\nu$. The emission of CH_3I and CD_3I in the course of dissociating has been studied by Kinsey and co-workers using the same techniques[4,20] as for O_3. For CH_3I/CD_3I the spectra consist of a series of C–I overtone transitions, and it is observed that the time dependence of the emission follows that of the laser, as should be the case, since the laser pulse is ≈10 ns, whereas the photodissociation proceeds on a femtosecond scale. The spectral pattern is consistent with a picture of the photodissociation process in which the initial motion stretches the C–I coordinate and in which subsequent motion[79] relaxes the CH_3 umbrella configuration to the planar CH_3.

(c) $NO_2^* \rightarrow NO + O$. In emission from NO_2*, intensity is observed[21] in both the symmetric stretch and bend, showing that in the upper state these modes are displaced from their equilibrium values. This information, together with ab initio calculations, provides evidence that the upper state is the $^2B_2$ state. The ratio of intensity in the bend to that in the stretch displays oscillations near the predissociation threshold. These oscillations die out at higher frequencies, showing that near threshold the excited complex lives for several vibrational periods and that lifetimes become shorter at frequencies beyond threshold.

V. van der Waals Molecules vs Transition Region Species

A. Location on the Surface

Excitation of a weakly bound van der Waals molecule is different from the excitation of an unbound species. van der Waals complexes are static species in thermal equilibrium with the reagents, and they are confined within some local minimum on the potential energy hypersurface. Excitation of a van der Waals complex will probe only this limited region of the ground-state potential energy hypersurface. Excitation to an excited hypersurface will allow the system to evolve on the *upper state, and information could be obtained about* the upper state in experiments similar to those of Kinsey et al., but the region probed on the lower surface will be limited. On the other hand, transition region species evolve in time along a multidimensional path on the journey from reagents to products. Excitation of a transition region species has the potential of probing the system along the reaction path *on the ground surface*. The reaction path does not correspond to the local minima of the van der Waals molecules.

This difference is shown by the experiments of Boivineau et al., in which excitation of the van der Waals complex[73] gives results *different* from the results obtained when a transition region species is excited. In {Xe···Cl_2}, the van der Waals complex formed in a supersonic expansion was excited[73b] in a two-photon process, and the XeCl* formed was vibrationally *cold*, whereas XeCl* formed in the two-photon excitation of a transition region species in the experiments of Setser et al.[68] was vibrationally warm. Similarly, two-photon excitation of the {Xe···Br_2} van der Waals complex[73a] produced XeBr*, whereas two-photon excitation of a transition region species did *not* produce XeBr*.[68]

B. Transience vs Equilibrium

van der Waals complexes should be present in equilibrium (albeit low) concentrations, even in nonreacting systems. They are *stationary states*, whereas transition region species are *transient*. The transient species will have far less time to interact with the field, so the transition probability will be much less than for a van der Waals complex.

Inoue, Ku, and Setser[15b] have calculated the equilibrium constant for formation of the {Xe–Cl} van der Waals complex to be 7×10^{-24} molecule^{-1} cm^3. They directly summed the v,J levels using an RKR potential: the vibration–rotational partition function is 614 at 298 K. (The rigid rotator–harmonic oscillator approximation greatly overestimates the partition function as 29 000). For 3 Torr of Xe, about one part per million of Cl is bound as {Xe···Cl}.

For the experiments on photoassociation of Xe,[54] we roughly estimate the equilibrium constant to be the same as for XeCl. The well depths are 195 vs 280 cm^{-1}, and r_e is 4.4 vs 3.2 Å. The Xe_2 well is thus considerably more shallow, but because of the larger r_e and smaller rotational spacing, the number of bound states is estimated to be roughly comparable. The experimental absorption coefficient is $\alpha = 4.3 \times 10^{-9}$ Torr^{-2} cm^{-1}, and if this process were to be explained as absorption by van der Waals molecules, the absorption cross section would be 0.005 Å^2. This is physically reasonable, even if the equilibrium concentration were somewhat underestimated. These experiments could thus be interpreted as the excitation of a van der Waals complex.

For the experiments[53] on Xe/Cl_2, we again roughly estimate the equilibrium constant for {Xe–Cl_2} to be equal to that for {Xe–Cl}, and for the experimental conditions at ≈180 Torr (23 Torr of Cl_2; 157 Torr of Xe) calculate the concentration of the van der Waals complex, {Xe–Cl_2} ≈ 3×10^{13}/cm^3, *corresponding to P ≈ 1*

mTorr. At this pressure 90% of the F_2 laser is observed to be absorbed over a path length of 50 cm, so the absorption coefficient is measured to be 0.046 cm^{-1}. If this is due to absorption by van der Waals complexes, the absorption cross section is ≈14 $Å^2$, which is large, but not unreasonably so.

We can also estimate[2] the steady-state concentration of transition region species for these cases. Assuming the activation energy for formation of the transition region species is zero, that the cross section for formation of the transition region species is roughly gas kinetic (10 $Å^2$), and that the lifetime $\tau \approx 1$ ps, we estimate the concentration of transition region species in both cases as $\approx 3 \times 10^{12}/cm^3$, roughly comparable to the concentration of van der Waals complexes. If the species responsible for absorbing the light in these experiments are transition region species, one thus expects absorption cross sections to be ≈0.005 and ≈14 $Å^2$ for $[Xe_2]$ and $[XeCl_2]$, respectively. But this calculation probably *overestimates* the steady-state concentration of transition region species since the lifetime may be much shorter (≈10 fs might be more appropriate). For $[XeCl_2]$, the reaction is endoergic, so the activation energy for forming a transition region species is likely not zero. We thus expect that few collisions will have sufficient energy to allow the reagents to approach to within bonding distances. Transition region species are thus likely to be even less populous than the van der Waals complexes, requiring very large (perhaps too large) absorption cross sections to explain the observations. These estimates thus strongly suggest that absorption by van der Waals molecules must be included as possible explanations for processes that might otherwise be thought of as excitation of a *transient* transition region species.

VI. Theory and Interpretation

Theoretical description of the detailed dynamics of a chemical reaction is extraordinarily difficult, even in the absence of a radiation field. As a consequence, we have sought to confine our attention to cases in which the radiation is weak enough to be used as a *probe* of the reaction dynamics.[80] The radiation thus needs to be weak enough to be only a perturbation on the reacting system, and in the following section, we explore the criteria for "weak enough" radiation. Theoretical interpretation of the results of such probe experiments has not yet been extensively developed, but it should follow along the lines of the theories developed for dark reaction suitably modified for the experimental conditions, and we review some of the qualitative aspects of the theory.

A. Transitions between Two Levels

Since lasers can easily supply power densities that are enormous by conventional standards, it is useful to consider the criteria for what constitutes "low" and "high" power.

For electric dipole transitions in a molecule between two levels q and p, the interaction energy W between the light and the molecule is

$$W = \mu \cdot \mathbf{E} = \mu_{pq} E_0 \tag{31}$$

where $\mu = \mu_{pq}$ is the transition dipole moment, and E_0 the electric field intensity due to the light. The radiation is normally treated as a *perturbation* on the molecular energy levels, which requires

$$\mu \cdot \mathbf{E} \ll \Delta W = W_q - W_p \tag{32}$$

where W_q and W_p are the energies of levels q and p. [Equation 32 is not very restrictive. For $\Delta W \approx 1$ GHz (rotational spacings), eq 32 gives laser powers ≈300 kW/cm^2. For $\Delta W \approx 16000$ cm^{-1} (visible), eq 32 is satisfied for powers up to $\approx 10^{17}$ W/cm^2, where multiphoton effects would predominate anyhow.]

If this molecule is irradiated at the transition frequency, $\omega_0 = (W_q - W_p)/h$, the standard result from time-dependent perturbation theory is that the intensity of a transition is

$$I = (\pi/2)\rho(\omega_0)\Omega^2\tau \tag{33}$$

where τ is the time the system is irradiated, $\rho(\omega_0)$ is the (constant) radiation density at ω_0, and the Rabi frequency, Ω, is $\Omega = 2\mu E_0/h$.

It is important to keep in mind that this assumes that the light is a *perturbation*, which requires that the probability of a transition is small.[81] This requires that

$$\Omega \ll 1/\tau \tag{34}$$

For *transient* species, τ is the time during which the system is in resonance with the applied field, and eq 34 shows that a given laser power can be considered a perturbation provided the irradiation time is sufficiently small. We will denote as "low" power that power where eq 34 is valid. Higher laser powers could still result in transitions between levels at a frequency ω_0, and multiphoton transitions must also be considered.[82]

In Table VII we have collected some representative Rabi frequencies for various laser powers. The power density $\langle S \rangle$, expressed in power/area, in an electromagnetic field $E = E_0 \cos(\omega t)$ is given by

$$\langle S \rangle = cE_0^2/(8\pi) \tag{35}$$

so the Rabi frequency is $\Omega = (8\pi\mu/h)[2\pi\langle S \rangle/c]^{1/2}$. For an allowed transition in, say, a sodium atom, the transition moment is high and for CW excitation, τ would be the flight time across the laser beam, ≈1 μs. For "low"-power excitation, eq 34 requires $\Omega < 1$ MHz, which, according to Table VII, is less than ≈100 $\mu W/cm^2$. For powers much above that, we expect the transition to appear "saturated". This is usually interpreted as having equal amounts of absorption and stimulated emission.

For excitation of very short-lived states, the "low"-power linear-in-time regime extends to much higher laser power. In the case of a chemically reacting system, we might expect a collision to last ≈1 ps and be in resonance with a radiation field for at most, say, 0.1 ps. Even if the transition moment is very high, inspection of Table VII shows that "low"-power behavior is expected up to ≈100 MW/cm^2. These light intensities are

TABLE VII Representative Values of Rabi Frequencies

power density W/cm^2	electric field, V/cm	$\Omega(\mu = 1$ D), MHz	$1/\Omega$, ps
0.001	0.9	6	58000
1.0	28	170	5800
1000	868	5500	180
10^6	27500	170000	6
10^8	275000	1700000	0.6

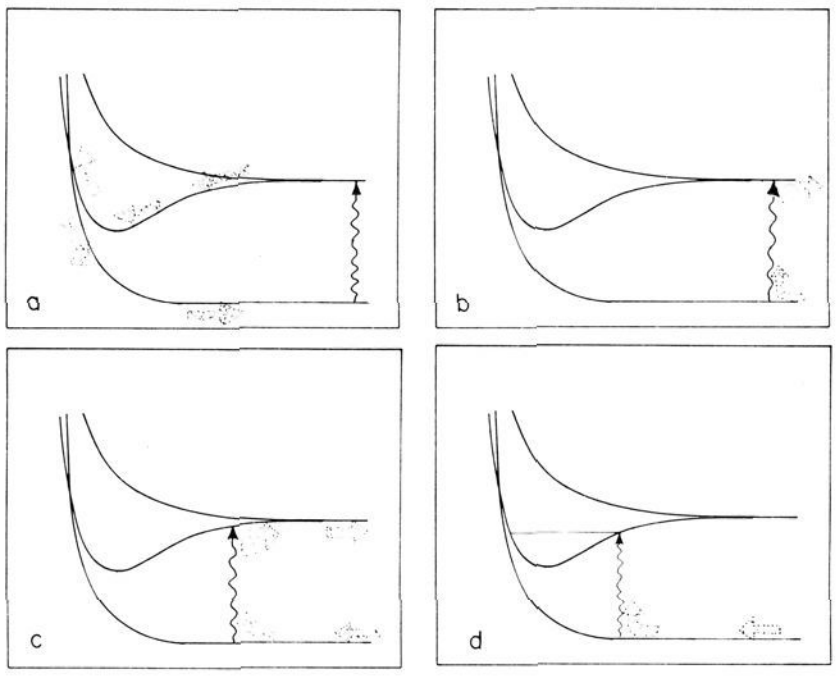

Figure 21. Schematic illustration of various optical/collision processes that occur in atomic systems. Absorption or emission of a photon is indicated by wiggly lines, and evolution of the diatom is indicated by the large shaded arrows. (a) Superleastic collision; (b) absorption in the wing of a resonance line; (c) collisional redistribution of radiation; (d) laser-assisted collision. (Adapted from: Hertel, I. *J. Phys., Colloq.* **1985**, *C1*, 37.)

certainly experimentally feasible,[83] but at intensities $\approx$100 MW/cm^2 we expect *formidable* experimental problems in distinguishing between "low"-power excitation of transition region species and multiphoton excitation of trace levels of impurities. As previously discussed, long-lived van der Waals molecules may behave like impurities because excitation of van der Waals molecules falls in the *high*-power regime. At powers so high that $\Omega = \omega_0$ one may also expect the ac–Stark effect to alter the molecular potentials involved.

B. Electronic Transitions

Electronic transitions take place between two electronic states. For collisions between atoms (or for electronic transitions in diatomic molecules), the potential energy in a given state, $V(r)$, is a function only of the internuclear distance, r, so $V(r)$ can conveniently be plotted vs r. A transition between electronic states can thus be represented pictorially as a transition between potential *curves*. Collisions that lead to chemical reaction, on the other hand, involve many more coordinates so that electronic transitions must be represented by transitions between multidimensional *surfaces*. Since multidimensional surfaces are difficult to visualize, reactions are frequently discussed in terms of various simplified potential *curves*. It is therefore useful to begin our discussion with a review of processes occurring on potential curves.

1. Potential Energy Curves

Transitions between potential curves for the atom–atom case form a basis for discussion of the more complicated cases involving chemical reaction. Figure 21 schematically illustrates a number of possible collisional phenomena occurring in the presence of radiation. Figure 21a shows a *superelastic collision*, wherein an excited atom can collide on an excited potential curve and undergo a nonradiative crossing to the ground curve. The electronic excitation is converted to translational excitation. Figure 21b shows a very weak, long-range collision with *absorption in the wings* of the resonance line. Panel c shows *collisional redistribution* of radiation in which absorption takes place during a closer collision where the energy separation is different from the asymptotic separation. If some translational energy is converted to electronic energy in the excited state, emission can occur when the atoms are far apart, corresponding to emission at the atomic resonance line. Panel d shows a *laser-assisted collision*, where absorption occurs in a region where the atoms strongly perturb one another and where the system is best viewed as a diatomic molecule. The fate of the system after absorption depends on the system; the process illustrated is photon-assisted association. (It should be noted that there is not a generally clear-cut distinction among these various processes because they span a range of collisional interactions.)

Detailed interpretation of the various processes described in Figure 21 relies implicitly and explicitly on the Born–Oppenheimer approximation that since electrons are much lighter and move much faster than nuclei, the motion of the electrons can be decoupled from the motion of the nuclei. Electronic transitions thus occur with the nuclear position and momenta essentially clamped, and the only transitions occurring are those in which the nuclear configuration is unaltered (so-called "vertical" transitions), so $h\nu = V\{\mathbf{r}_f\} - V\{\mathbf{r}_i\}$ and $\{\mathbf{r}_f\} = \{\mathbf{r}_i\}$. The transition probability should depend on the Franck–Condon factors, or the overlap integrals, between the two states. This is well-known for bound–bound transitions, and it is also experimentally observed for the unbound cases discussed here (see also ref 62). For example, Scheingraber and Vidal[56] found that the discrete and continuous bands of the Mg_2 A–X transition could be quantitatively interpreted in terms of the Franck–Condon factors, and similar results were obtained for Ca_2,[57] Sr_2,[58] NaAr,[85] and the rare-gas halides.[84] Likewise, the interference maxima observed in the photoassociation of Xe + Cl[15,17,55] and Hg + Hg[59] can be interpreted in terms of the Franck–Condon factors. The Franck–Condon approximation is the workhorse of the quasi-static theory of atomic line broadening, and these spectra are well described in this approximation.[86]

Some attention has been drawn to "non-Franck–Condon" transitions because emission spectra of molecular ions, such as O_2^+, formed in Penning ionization collisions with He(2 ^{3}S) metastables exhibit intensities radically different from photoionization spectra.[87] These transitions should not be expected to be "vertical" because the O_2 and O_2^+ potential *curves* are insufficient to describe the process. Because of the impact of the heavy He nucleus, one needs to consider transitions from a [HeO_2] *surface* to a [HeO_2^+] *surface*. We expect these processes to be well described by the Franck–Condon approximation if transitions between the triatomic *surfaces* are considered.

Kleiber et al.[13] have used a quasi-atomic model to estimate the absorption profiles in the photon-assisted reaction Mg + H_2 + $h\nu \rightarrow$ MgH + H. Using ab initio SCF–CI potentials[88] (calculated for either C_{2v} or $C_{\infty v}$ geometry with the H_2 internuclear distance fixed at its equilibrium value), they estimate transition probabilities to each of several excited potential curves representing reagents. They assume that a transition to a

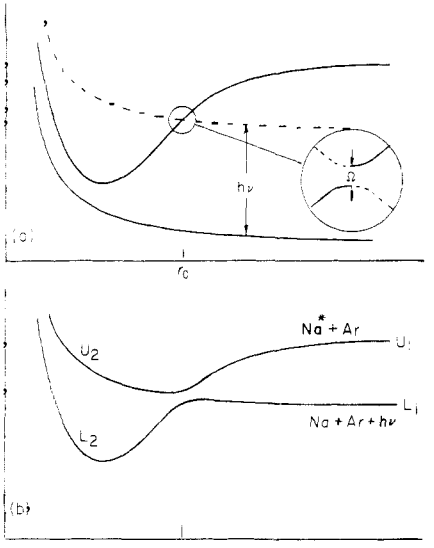

Figure 22. Schematic potential curves for the collision system Na + Ar. (a) The laser of frequency ν shifts the ground-state potential curve up a distance $h\nu$, where it intersects the excited state in an avoided crossing at r_c. The avoided crossing region is enlarged for clarity. (b) Electronic-field curves resulting from avoided crossing in (a). (Adapted from ref 91.)

bound or quasi-bound upper curve leads to reaction. (To obtain agreement with experiments, it was necessary to postulate that one repulsive upper state also leads to reaction.) This "atomic entrance channel" approach is reasonable since reaction of Mg* is known to be facile.[72] As previously mentioned, endoergic reactions may have an activation energy, making close nuclear approach unlikely. Optical probing of such a reaction will thus give information mostly about the entrance channel. In this case, the entrance channel corresponds to the region where the H_2 internuclear distance has not yet changed much. This model is in rough accord with experiment as shown in Figure 15, but there are clearly gaps between the theory and the experiments.

2. Dressed States

Absorption of a photon by a quasi-molecule may be viewed in an alternative fashion. Figure 22 schematically shows the Na + Ar collision system with a photon corresponding to a resonance between the ground excited states which would occur at r_c. The dashed line is the ground-state curve moved up by the energy of the photon and represents the system {Na + Ar + $h\nu$}. This curve is known as a dressed curve[89] or an electronic-field curve[90] and results in an avoided crossing with the upper state at r_c. The energy gap between the two curves becomes larger as the light intensity is increased, and the crossing radius depends on $h\nu$.

The process of light absorption may now be viewed as a curve-crossing process, and is usually described in terms of the Landau–Zener model, where the probability p of jumping across the gap is

$$p = e^{-W} \tag{36}$$

where

$$W = \frac{h\Omega^2}{v|\partial V_2/\partial r - \partial V_1/\partial r|_{r_c}} \tag{37}$$

v is the speed, $h\Omega/2\pi$ is the off-diagonal Hamiltonian matrix element, and $\partial V_i/\partial r|_{r_c}$ is the slope of the ith curve at the crossing, r_c. Thus a jump will be favored by a slow traversal of the region (leading to longer exposure to the light), and favored if the curves are parallel (leading to larger FC overlap).

Absorption in the Na + Ar collision system occurs in one of two ways: (1) If the atoms approach on the curve marked "L_1" in Figure 22b, adiabatically traverse the crossing region at r_c to curve "L_2", and then make a *nonadiabatic* traversal of the crossing on the way out, they will end up on curve "U_1" corresponding to Na* + Ar. (2) If the atoms jump to "U_2" on the way in and then make an adiabatic transition on the way out, they also end up on curve "U_1", corresponding to Na* + Ar. In either case, one jump and one adiabatic transition produce excited products.

The dressed-state view is useful at high light intensity where the avoided crossing is large and the resulting potentials can support bound species.[3] This picture is also particularly appropriate for discussing light pulses, which are short in comparison to the collision time.[91] If the region of the avoided crossing is traversed at all, it is traversed once on the way into the collision and once on the way out, so if the light is on for both crossings (long pulse), the probability of exciting an atom is the probability of one jump and one adiabatic transition, or

$$P_{\text{long}} = 2p(1 - p) \tag{38}$$

where p is given by eq 36. In contrast, if the light pulse is short compared to the time between traversals (≈1–2 ps) the Na atom may be dressed by the light field for only *one* traversal. If the pulse is turned off before the second traversal of r_c, the dressed state disappears, and the Na may be trapped on the upper curve. The probability of excitation for a short pulse is thus the probability of *one* adiabatic transition, so

$$P_{\text{short}} = 1 - p \tag{39}$$

Since p decreases with laser intensity, $P_{\text{short}} \rightarrow 1$, and $P_{\text{long}} \rightarrow 0$. This greater efficiency of excitation predicted for short pulses has been experimentally observed by Sizer and Raymer[91] for 1.6-ps pulses in the Na + Ar system.

3. Potential Energy Surfaces

In the process of chemical reaction, the nuclei start with an initial set of nuclear coordinates $\{\mathbf{r}_i\}$ corresponding to reagents and evolve to a final set of coordinates $\{\mathbf{r}_f\}$ corresponding to products. This evolution, $\mathbf{r}(t)$, is most conveniently described classically as a trajectory on a potential energy hypersurface in some n-dimensional space. *Calculation* of $\mathbf{r}(t)$ requires that the classical equations of motion must be solved on the potential energy surface, $V(\mathbf{r})$. Unfortunately, with the possible exception of H_3, the correct $V(\mathbf{r})$ is not known, and one of the problems in theoretical chemical kinetics is calculation of $V(\mathbf{r})$. Nonetheless, *insight* into the reaction dynamics has been obtained from *model* potential surfaces.

The simplest chemical reaction, A + BC → AB + C, requires three coordinates, so four dimensions are required to display the potential energy surface (pes). For display purposes, it is customary to simplify the reaction to one in which the three atoms are constrained to a *line*

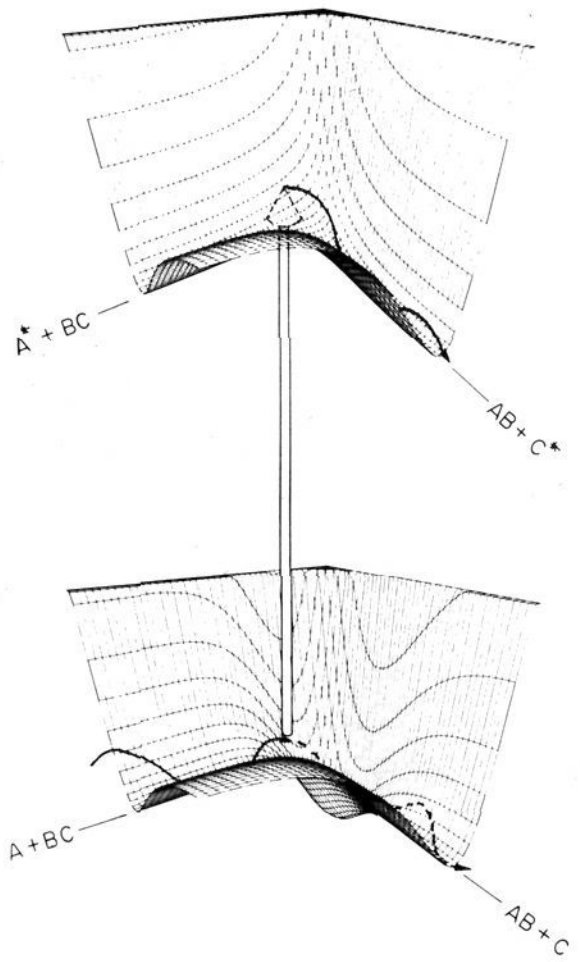

Figure 23. *Schematic* representation of an electronic transition occurring during a chemical reaction. A possible reagent approach is indicated by the trajectory on the lower surface; excitation to the upper surface will occur when the lower trajectory explores a region where the energy separation between the two surfaces corresponds to the photon energy.

and the potential can be presented as energy contours on a two-dimensional page. This approach has some theoretical justification because calculations show that the activation energy for the H + H_2 reaction has a minimum in the collinear configuration.

The effect on a trajectory of an absorption (emission) of a photon depends on the spectral region involved. In the infrared, for example, vibrational motion of the system would be changed, but the trajectory would remain on the same potential energy surface. Orel and Miller[92] have suggested that during the H + H_2 reaction the transition region species H_2···H is not symmetric and could thus absorb in the IR. This would have the result of exciting a transient absorption in the asymmetric stretch of the H_3 system to provide an infrared spectroscopy of transition region species. Collision-induced absorption in the IR is well-known, of course,[25,93] but to our knowledge, IR transitions during reactive events have not yet been experimentally observed.

Absorption in the visible or UV will result in a transition to a *new* potential surface. A schematic illustration of this process is shown in Figure 23. The overall process depends on *two* potential surfaces, the energy separation between the surfaces, and the dynamics on each of the two surfaces.

If a collision occurs in a radiation field of frequency ν, a transition will occur in the semiclassical approximation when the trajectory on the ground state samples a nuclear configuration which gives an energy separation between the two surfaces equal to $h\nu$. As the system traverses the ground-state pes, the trajectory will thus "tune" the system into resonance with the applied radiation field. The nuclear configurations which are excited will depend on the frequency ν. For a given frequency ν this may occur at several nuclear configurations, and the observed spectrum will not have a single-valued correspondence with the separation between the potential energy surfaces. Moreover, the observed spectrum will be the result of an average over initial energies, impact parameters, and molecular orientations. (The transition moment is also expected to vary with nuclear configuration.) Nonetheless, the spectrum will provide information about the energy separation between the surfaces and about the dynamics on the initial surface.

Polanyi and co-workers have computed classical trajectories for model systems emitting in the course of reaction[94] (section IV.B), and for collinear and 3-D absorption in the H + H_2 system.[95] These calculations suggest that features can appear in the spectrum which will correlate with certain types of motion on the initial surface and with certain relationships between the surfaces. For example, if the separation between the surfaces is constant (i.e., if the surfaces are "parallel") over a range of nuclear configurations, a number of different configurations can absorb at basically the same frequency, giving a large contribution to the absorption spectrum at that frequency, an effect similar to an atomic "satellite". (This is always the case in the asymptotes where nearly unperturbed resonances are observed.) The transition probability will depend on the time the system spends in resonance with the radiation field, so areas on the surface that are slowly traversed or where trajectories cause probability to "pool" will make larger contributions to the spectrum than others. Increased energy in the colliding pair results in shorter traversal times, so the intensity of the spectrum is expected to decrease, and the increased energy should simultaneously shift the spectrum to the red. A few quantum mechanical calculations for [H_3] suggest, as might be expected, that the classical treatment is very broadly correct, but omits structure present in the quantum mechanical calculation.[96-99]

VII. Conclusions

Light absorption during chemical reaction is a special, very complex, subset of photon/collision events which cover an extended range of interactions. The most gentle, long-range collisions affect the central portion of an atomic line[100] whereas "*hard-core collisions*" capable of leading to chemical reaction manifest themselves in the extreme wings (large perturbations) of an atomic line.

Experiments that show that light can be absorbed or emitted *during* a collision between two *atoms* are now well documented, and theoretical descriptions of these *nonreactive* processes are reasonably well developed. Similar experiments on collisions between chemically reactive species have also been performed, and the evidence suggests that transition region species in chemical reaction can also undergo optical transitions. These reactive events are much more complicated than collisions between atoms, and the field is only beginning to develop. Theory is in its infancy, and the experimental results are fragmentary.

The original intent in studying reactions in laser fields was to develop a spectroscopy of the transition region and to probe chemical reactions during the reaction process. This is still a valid objective. Spectra that are obtained will depend on the two potential energy sur-

faces involved and on the dynamics of reaction on the initial surface. While it does not seem likely at this time that the experimental data can be inverted to give potential energy surfaces, the model trajectory calculations suggest that valuable information about the reaction process can still be obtained. It does not require much imagination to suggest that if conventional measurements (rate, angular distributions, etc.) made on the asymptotic channels of a reaction are useful in elucidating the dynamics, measurements made *during* the reaction process itself will add greatly to the store of useful information available.

VIII. A Postscript

Material included in this review has been, by and large, restricted to work that had been published prior to January 1987, and I apologize for any work that has been overlooked. Several new investigations have been brought to my attention as this article is being finished, and these are mentioned here.

Neumark and co-workers[101] have initiated experiments to probe possible long-lived vibrational states on the Cl + HCl potential surface in the transition region. The translational energy of electrons photodetached from the stable anion $ClHCl^-$ is apparently due to neutral states lying above the Cl + HCl asymptote. Somewhat similar techniques have also been used by Morgner and his collaborators.[102] They have measured spectra of the electrons emitted from complexes of halogens and metastable rare gases, and after considerable modeling, some information about the reactive surface has been inferred.

Yamashita and Morokuma have calculated absorption spectra for the KClNa system.[103] They calculate MRSD–CI potential surfaces for the ground and excited surfaces and (following ref 94) assumed the absorption intensity is proportional to the density of KClNa classical trajectories on the ground-state potential surface and to the square of the transition dipole moment at the various geometries. (All earlier calculations on other systems assumed the transition dipole moment was a constant.) They conclude that the spectrum consists of two broad bands arising from transitions to the first and second excited electronic states and suggest that it may be possible to probe quasi-bound vibrational states on the two excited electronic surfaces.

Zewail and his colleagues[104] have just reported experiments in which a transition region species is interrogated in real time. They prepare ICN in a repulsive state with a femtosecond pulse and then, using a second such pulse, interrogate the molecule as it is in the process of falling apart.

IX. Acknowledgments

I gratefully acknowledge financial support received from the National Science Foundation and from The Robert A. Welch Foundation. I thank Alan Gallagher, Jim Kinsey, Paul Kleiber, John Polanyi, and Don Setser for helpful comments and for permission to reproduce their figures. I thank P. Hering, K. Morokuma, D. Neumark, M. G. Raymer, and A. Zewail for communication of preliminary results and thank John Hutchinson and Ken Marshall for assistance in constructing Figure 23. Thanks are especially due to my colleagues at Rice, Bob Curl, Howard Carman, Leon Phillips, Jim Spence, Syd Ulvick, and Mike Barnes, for bearing with me and for participating in many lively, but never quite bloody, discussions.

References

(1) Leone, S. R. "State Resolved Molecular Reaction Dynamics". *Annu. Rev. Phys. Chem.* **1984**, *35*, 109.
(2) Brooks, P. R.; Curl, R. F.; Maguire, T. C. "Experimental Observations regarding Transition States". *Ber. Bunsen-Ges. Phys. Chem.* **1982**, *86*, 401.
(3) Foth, H. J.; Polanyi, J. C.; Telle, H. H. "Emission from Molecules and Reaction Intermediates in the Process of Falling Apart". *J. Phys. Chem.* **1982**, *86*, 5027.
(4) Imre, D.; Kinsey, J. L.; Sinha, A.; Krenos, J. "Chemical Dynamics Studied by Emission Spectroscopy of Dissociating Molecules". *J. Phys. Chem.* **1984**, *88*, 3956.
(5) Kneba, M.; Wolfrum, J. "Bimolecular Reactions of Vibrational Excited Molecules". *Annu. Rev. Phys. Chem.* **1980**, *31*, 47.
(6) Altkorn, R.; Zare, R. N. "Effects of Saturation on Laser-Induced Fluorescence Measurements of Population and Polarization". *Annu. Rev. Phys. Chem.* **1984**, *35*, 265.
(7) Arnoldus, H. F.; George, T. F.; Lam, K. S.; Scipione, J. F.; DeVries, P. L.; Yuan, J. M. "Recent Progress in the Theory of Laser-Assisted Reactions". *Laser Applications in Physical Chemistry*; Evan, D. K., Ed.; Marcel Dekker: New York, **1986** and references cited therein.
(8) Kleiber, P. D.; Burnett, K.; Cooper, J. "Observation of the Modification of "Optical" Collision Dynamics in Intense Laser Fields". *Phys. Rev. Lett.* **1981**, *47*, 1595.
(9) Hering, P.; Brooks, P. R.; Curl, R. F., Jr.; Judson, R. S.; Lowe, R. S. "Chemiluminescent Reaction Channel Opened by Photon Absorption During Collision". *Phys. Rev. Lett.* **1980**, *44*, 687.
(10) (a) Maguire, T. C.; Brooks, P. R.; Curl, R. F. "Photoexcitation of the KNaCl Reaction Complex". *Phys. Rev. Lett.* **1983**, *50*, 1918. (b) Maguire, T. C.; Brooks, P. R.; Curl, R. F.; Spence, J. H.; Ulvick, S. "Photoexcitation of Reaction Complexes in the Reaction K + NaCl → KCl + Na". *J. Chem. Phys.* **1986**, *85*, 844.
(11) Kaesdorf, S.; Brooks, P. R.; Curl, R. J.; Spence, J. H.; Ulvick, S. J. "Observation of the laser assisted reaction K + NaCl + $h\nu$ → KCl + Na* using K atoms selected by a hexapole magnetic field". *Phys. Rev. A* **1986**, *A34*, 4418.
(12) Helvajian, H.; Marquardt, C. L. "Collision induced IR absorption in gas phase $Hg(6\ ^3P_1)$ + $HgBr(1\ ^1\Sigma_g+)$ reactions: Enhancement of the HgBr ($B\ ^2\Sigma+$) product channel". *J. Chem. Phys.* **1985**, *83*, 3334.
(13) (a) Kleiber, P. D.; Lyyra, A. M.; Sando, K. M.; Henegham, S. P.; Stwalley, W. C. "Far Wing Absorption Profiles of A Reactive Collision: Mg + H_2". *Phys. Rev. Lett.* **1985**, *54*, 2003. (b) Kleiber, P. D.; Lyyra, A. M.; Sando, K. M.; Zafiropulos, V.; Stwalley, W. C. "Reactive collision dynamics by far wing laser scattering: Mg + H_2". *J. Chem. Phys.* **1986**, *85*, 5493.
(14) (a) Polak-Dingels, P.; Bonanno, R.; Keller, J.; Weiner, J. "Direct Observation of a two-photon radiative ionization collision in crossed Ba-Na Atomic Beams". *J. Phys. B* **1982**, *15*, L41. (b) Polak-Dingels, P.; Keller, J.; Weiner, J.; Gauthier, J. C.; Bras, N. "Observation of laser-induced associative ionization in crossed-beam Na + Li collisions". *Phys. Rev. A* **1981**, *A24*, 1107.
(15) (a) Inoue, G.; Ku, J. K.; Setser, D. W. *J. Chem. Phys.* **1982**, *76*, 733. (b) Inoue, G.; Ku, J. K.; Setser, D. W. "Photoassociative laser-induced fluorescence of XeCl* and kinetics of XeCl(B) and XeCl(C) in Xe". *J. Chem. Phys.* **1984**, *80*, 6006.
(16) McCown, A. W.; Eden, J. G. "Ultraviolet photoassociation production of XeCl(B,C) molecules in Xe/Cl_2 gas mixtures. Radiative lifetime of $Xe_2Cl(4\ ^2G)$". *J. Chem. Phys.* **1984**, *81*, 2933.
(17) Ku, J. K.; Setser, D. W.; Oba, D. "Laser Photoassociation of Xe and Br(2P3/2) atoms and generation of aligned XeBr(B) molecules". *Chem. Phys. Lett.* **1984**, *109*, 429.
(18) (a) Arrowsmith, P.; Bartoszek, F. E.; Bly, S. H. P.; Carrington, T., Jr.; Charters, P. E.; Polanyi, J. C. "Chemiluminescence during the course of a reactive encounter: F + Na_2 → FNaNa** → NaF + Na*". *J. Chem. Phys.* **1980**, *73*, 5895. (b) Arrowsmith, P.; Bly, S. H. P.; Charters, P. E.; Polanyi, J. C. "Spectroscopy of the transition state II: F + Na_2 → FNaNa** → NaF + Na*". *J. Chem. Phys.* **1983**, *79*, 283.
(19) Imre, D. G.; Kinsey, J. L.; Field, R. W.; Katayama, D. H. "Spectroscopic Characterization of Repulsive Potential Energy Surfaces: Fluorescent Spectrum of Ozone". *J. Phys. Chem.* **1984**, *86*, 2564.
(20) Hale, M. O.; Galica, G. E.; Glogover, S. G.; Kinsey, J. L. "Emission Spectroscopy of Photodissociating CH_3I and

CD_3I^v. *J. Phys. Chem.* **1986**, *90*, 4997.
(21) Rohlfing, E. A.; Valentini, J. J. "Structure & Predissociation Dynamics of Electronically excited NO_2: A resonance Raman Study". *J. Chem. Phys.* **1985**, *83*, 521.
(22) Allard, N.; Kielkopf, J. "The Effect of Neutral non-resonant collisions on atomic spectral lines". *Rev. Mod. Phys.* **1982**, *54*, 1103.
(23) In order to avoid cumbersome repetition, we discuss this only in terms of emission, but similar considerations apply equally well to absorption.
(24) The transition will not be observed *exactly* at the zero-pressure frequency limit. The transition moment is a function of internuclear distance and for a forbidden transition must vanish at line center, corresponding to asymptotically separated atoms. Transitions thus correspond to perturbed atoms and the line will not peak exactly at ν_0.
(25) Crawford, M. F.; Welsh, H. L.; Locke, J. L. "Infra-red absorption of O_2 and N_2 induced by intermolecular forces". *Phys. Rev.* **1949**, *75*, 1607.
(26) Su, R. T. M.; Bevan, J. W.; Curl, R. F., Jr. "Laser excitation of the 5d $^2D_{5/2}$ level of Cs during collision with rare gas atoms". *Chem. Phys. Lett.* **1976**, *43*, 162.
(27) Hedges, R. E. M.; Drummond, D. L.; Gallagher, A. "Extreme-Wing Line Broadening and Cs Inert-Gas Potentials". *Phys. Rev. A* **1972**, *A6*, 1579.
(28) (a) Ottinger, Ch.; Scheps, R.; York, G. W.; Gallagher, A. "Broadening of the Rb resonance lines by the noble gases". *Phys. Rev. A* **1975**, *A11*, 1815. (b) York, G.; Scheps, R.; Gallagher, A. "Continuum Radiation & potentials of Na Noble gas molecules". *J. Chem. Phys.* **1975**, *63*, 1052. (c) Carrington, C. G.; Gallagher, A. "Satellite Bands of Rubidium broaned by noble gases". *Phys. Rev. A* **1974**, *A10*, 1464. (d) Chatham, R. H.; Gallagher, A.; Lewis, E. L. "Broadening of the sodium D lines by rare gases". *J. Phys.* **1980**, *B13*, 17.
(29) This nomenclature is unfortunate for our purposes, since a "hard core" *collision* usually refers to a rather violent (small impact parameter) collision in which the atoms behave almost as hard spheres. "Impact" in this context suggests such a collision.
(30) Gallagher, A. "The Spectra of Colliding Atoms". *Atomic Physics*; zu Putlitz, G., et al., Eds.; Plenum: New York, 1975.
(31) Carlsten, J. L.; Szöke, A.; Raymer, M. G. "Collisional redistribution and saturation of near resonance scattered light". *Phys. Rev. A* **1977**, *A15*, 1029.
(32) Thomann, P.; Burnett, K.; Cooper, J. "Observation of Dynamic Correlations in Collisional Redistribution and Depolarization of Light". *Phys. Rev. Lett.* **1980**, *45*, 1325.
(33) Alford, W. J.; Burnett, K.; Cooper, J. "Polarization of collisionally redistributed light from the far wings of Strontium-rare gas collisions". *Phys. Rev. A* **1983**, *A27*, 1310.
(34) (a) Alford, W. J.; Anderson, N.; Burnett, K.; Cooper, J. "Collisional Redistribution of Light: Far wing line shapes & Polarization for the Ba-(Xe,Ar) systems". *Phys. Rev. A* **1984**, *A30*, 2366. (b) Alford, W. J.; Anderson, N.; Belsley, M.; Cooper, J.; Warrington, D. M.; Burnett, K. "Collisional redistribution of circularly polarized light in Barium perturbed by Argon". *Phys. Rev. A* **1985**, *A31*, 3012.
(35) Havey, M. D.; Copeland, G. E.; Wang, W. J. "Fine-structure transitions Occurring in Collisional *Redistribution* of Light". *Phys. Rev. Lett.* **1983**, *50*, 1767.
(36) Kulander, K.; Rebentrost, F. "Collisional Redistribution & f.s. transitions in Na-Ar". *J. Chem. Phys.* **1984**, *80*, 5623.
(37) Rebentrost, F. "Thermal fluorescence ratios in non-resonant excitation of Na-Ar collision pairs". *J. Phys.* **1986**, *B19*, L121.
(38) Gudzenko, L. I.; Yakovlenko, S. I. "Radiative Collisions". *Sov. Phys.—JETP (Engl. Transl.)* **1972**, *35*, 877.
(39) Yakovlenko, S. I. "Laser Induced Radiative Collisions". *Sov. J. Quantum Electron. (Engl. Transl.)* **1978**, *8*, 151.
(40) Falcone, R. W.; Green, W. R.; White, J. C.; Young, J. F.; Harris, S. E. "Observation of laser-induced inelastic collisions". *Phys. Rev. A* **1977**, *A15*, 1333.
(41) Harris, S. E.; White, J. C. "Numerical Analysis of Laser Induced Inelastic Collisions". *IEEE J. Quantum. Electron.* **1977**, *QE13*, 972.
(42) Harris, S. E.; Young, J. F.; Green, W. R.; Falcone, R. W.; Lukasik, J.; White, J. C.; Willison, J. R.; Wright, M. D.; Zdasiuk, G. A. "Laser Induced Collisional & Radiative Energy Transfer". *Laser Spectroscopy IV*; Walther, H., Rothe, K. W., Eds.; Springer-Verlag: Berlin, 1979.
(43) (a) Green, W. R.; Lukasik, J.; Willison, J. R.; Wright, M. D.; Young, J. F.; Harris, S. E. "Measurement of Large Cross Sections for Laser-induced Collisions". *Phys. Rev. Lett.* **1979**, *42*, 970. (b) Green, W. R.; Wright, M. D.; Lukasik, J.; Young, J. F.; Harris, S. E. "Observation of a laser-induced dipole quadrupole collision". *Opt. Lett.* **1979**, *4*, 265. (c) Green, W. R.; Wright, M. D.; Young, J. F.; Harris, S. E. "Laser-induced charge transfer to an excited Ionic state". *Phys. Rev. Lett.* **1979**, *43*, 120.
(44) (a) White, J. C.; Zdasiuk, G. A.; Young, J. F.; Harris, S. E. "Observation of Radiative Collisional Fluorescence". *Phys. Rev. Lett.* **1978**, *41*, 1709. (b) White, J. C.; Zdasiuk, G. A.; Young, J. F.; Harris, S. E. "Observation of Atomic Pair absorption with an incoherent source". *Opt. Lett.* **1979**, *4*, 137.
(45) White, J. C. "Stimulated-absorption and spontaneous-emission studies of laser-induced dipole quadrupole collisions". *Phys. Rev. A* **1981**, *A23*, 1698.
(46) Brechignac, C.; Cahuzac, Ph.; Toschek, P. E. "High Resolution Studies on laser-induced collisional energy transfer profiles". *Phys. Rev. A* **1980**, *A21*, 1969.
(47) Lukasik, J.; Wallace, S. C. "Laser-assisted intermolecular energy transfer between electronic states of CO in the VUV". *Phys. Rev. Lett.* **1981**, *47*, 240.
(48) Brêchignac, C.; Cahuzac, Ph.; Debarre, A. "Laser induced Collisional energy transfer: High resolution studies & coherence effects in dipole-dipole interaction". *J. Phys., Colloq.* **1985**, *C1*, 107.
(49) LICET. This phenomenon is also called a "radiative collision" or referred to as "radiatively aided inelastic collisions" (RAIC).
(50) (a) Cunha, S. L.; Ulivi, L.; Hering, P.; Kompa, K. L. "CARS studies of NaH_2 collision rates". Private communication, 1985. (b) Hering, P.; Cunha, S. L.; Kompa, K. L. "CARS Study of the Energy Partitioning in the Na(3P)-H_2 Collision Pair with Red Wing Excitation". Personal communication, 1987.
(51) Kamke, W.; Kamke, B.; Hertel, I.; Gallagher, A. "Fluorescence of the Na*-N_2 collision Complex". *J. Chem. Phys.* **1984**, *80*, 4879.
(52) Gallagher, A.; Holstein, T. "Collision-induced absorption in atomic electronic transitions". *Phys. Rev. A* **1977**, *A16*, 2413.
(53) Grieneisen, H. P.; Zue-Jing, H.; Kompa, K. L. "Collision Complex Excitation in Chlorine-Doped Xenon". *Chem. Phys. Lett.* **1981**, *82*, 421.
(54) Grieneisen, H. P.; Hohla, K.; Kompa, K. L. "Formation of Xe_2* by collision-pair absorption at 158 nm". *Opt. Commun.* **1981**, *37*, 97.
(55) Setser, D. W.; Ku, J. "Reactions between Xenon and Halogen Containing Molecules". *Photophysics and Photochemistry above 6 eV*; Lahmani, F., Ed.; Elsevier: Amsterdam, 1985; p 621.
(56) Scheingraber, H.; Vidal, C. R. "Discrete and Continuous Franck–Condon Factors of the Mg_2 $A^1\Sigma_u$–$X^1\Sigma_g$ System and their *J* Dependence". *J. Chem. Phys.* **1977**, *66*, 3694.
(57) Vidal, C. R. "The molecular constants and potential energy curves of the Ca_2 $A^1\Sigma_u$–$X^1\Sigma_g$ system from laser induced fluorescence". *J. Chem. Phys.* **1980**, *72*, 1864.
(58) Gerber, G.; Moller, R.; Schneider, H. "Laser induced bound-bound and bound-continuum emission of the Sr_2 $A^1\Sigma_u$–$X^1\Sigma_g$ system". *J. Chem. Phys.* **1984**, *81*, 1538.
(59) (a) Ehrlich, D. J.; Osgood, R. M., Jr. "Condon Internal Diffraction in the O_u^+–O_g^+ Fluorescence of Photoassociated Hg_2". *Phys. Rev. Lett.* **1978**, *41*, 547. (b) Ehrlich, D. J.; Osgood, R. M., Jr. "Collision-induced Predissociation in Photoassociated Hg_2". *Chem. Phys. Lett.* **1979**, *61*, 150.
(60) Wilcomb, B. E.; Burnham, R. "Nonresonant collision-induced absorption in Xe/Cl_2 mixtures". *J. Chem. Phys.* **1981**, *74*, 6784.
(61) (a) Dubov, V. S.; Gudzenko, L. I.; Gurvich, L. V.; Iakovlenko, S. E. "Experimental Detection of Chemical Radiative Collisions". *Chem. Phys. Lett.* **1978**, *53*, 170. (b) Dubov, V. S.; Lapsker, Y. E.; Samoilova, A. N.; Gurvich, L. V. "Experimental detection of Chemical Radiative Collisions in Xe + Cl_2". *Chem. Phys. Lett.* **1981**, *83*, 518.
(62) Tellinghuisen, J. "The Franck–Condon Principle in Bound–Free Transitions". In *Photodissociation and Photoionization*; Lawley, K., Ed.; Wiley: New York, 1985.
(63) Polak-Dingels, P.; Delpech, J.-F.; Weiner, J. "Observation of Structure in Laser-Induced Penning and Associative Ionization in Crossed-Beam Na + Na Collisions". *Phys. Rev. Lett.* **1980**, *44*, 1663.
(64) Boulmer, J.; Weiner, J. "Production of Na_2^+ by crossed beam collisions in the presence of intense, non-resonant radiation". *Phys. Rev. A* **1983**, *A27*, 2817.
(65) Keller, J.; Weiner, J. "Multiphoton Ionization Spectroscopy of the Sodium Dimer". *Phys. Rev. A* **1984**, *A30*, 213.
(66) v. Hellfeld, A.; Caddick, J.; Weiner, J. "Observation of Laser-Induced Penning and Associative Ionization in Li–Li Collisions". *Phys. Rev. Lett.* **1978**, *40*, 1369.
(67) Pradel, P.; Monchicourt, P.; Dubreuil, D.; Heuze, J.; Laucagne, J. J.; Spiess, G. "Observation of a Laser-Assisted Ionization of the He ($2\ ^1S$,$2\ ^3S$) + He ($1\ ^1S$) Collision System Involving a Bound-Free Transition". *Phys. Rev. Lett.* **1985**, *54*, 2600.
(68) Ku, J. K.; Inoue, G.; Setser, D. W. "Two-Photon Laser-Assisted Reaction with Xe/Cl_2 to form XeCl* and with Xe/ICl to form XeCl* and XeI*". *J. Phys. Chem.* **1983**, *87*, 2787.
(69) Bullitt, M. K.; Fisher, G. H.; Kinsey, J. "Molecular Beam Reactions of Potassium Atoms with $ZnCl_2$, ZnI_2, CdI_2, $HgBr_2$, and HgI_2". *J. Chem. Phys.* **1974**, *60*, 428.
(70) Maguire, T. C. Ph.D. Thesis, Rice University, 1984.

(71) Safron, S. Ph.D. Thesis, Harvard University, 1969.
(72) Breckenridge, W. H.; Umemoto, H. *J. Chem. Phys.* **1981**, *75*, 698; **1984**, *80*, 4168.
(73) (a) Boivineau, M.; LeCalve, J.; Castex, M. C.; Jouvet, C. "Formation of the Xe-Br* excimer by double optical excitation of the Xe-Br_2 van der Waals complex". *J. Chem. Phys.* **1986**, *84*, 4712. (b) Boivineau, M.; LeCalvé, J.; Castex, M. C.; Jouvet, C. "Role of the entrance channel on the product internal energy distribution in the reaction Xe-Cl_2* → XeCl* + Cl". *Chem. Phys. Lett.* **1986**, *84*, 4712.
(74) Jouvet, C.; Soep, B. "Electronic relaxation induced by dissociation of a van der Waals complex: (Hg-N_2)*($^3P_1$) → Hg($^3P_0$) + N_2". *J. Chem. Phys.* **1984**, *80*, 2229.
(75) Jouvet, C.; Soep, B. "Direct Observation of the transition state of a photochemical reaction, the Hg $^3P_1$, Cl_2 system". *J. Phys., Colloque* **1985**, *C1*, 313.
(76) Breckenridge, W. H.; Jouvet, C.; Soep, B. "Orbitally selective chemical reaction in Hg-H_2 van der Waals complexes". *J. Chem. Phys.* **1986**, *84*, 1443.
(77) (a) Heller, E. J. "The semiclassical way to molecular spectroscopy". *Acc. Chem. Res.* **1982**, *86*, 862. (b) Heller, E. J.; Sundberg, R. L.; Tannor, D. "Simple Aspects of Raman Scattering". *J. Phys. Chem.* **1982**, *86*, 1822.
(78) Hay, P. J.; Pack, R. T.; Walter, R. B.; Heller, E. J. *J. Phys. Chem.* **1982**, *86*, 862.
(79) Sundberg, R. L.; Imre, D.; Hale, M. O.; Kinsey, J. L.; Coalson, R. D. "Emission Spectroscopy of Photodissociating Molecules: A Collinear Model for CH_3I and CD_3I". *J. Phys. Chem.* **1986**, *90*, 5001.
(80) Light intensities high enough to *alter* the molecular potentials during a collision via the ac–Stark effect are easily obtainable in calculations (see, for example: Ho, T. S.; Chu, S. I.; Laughlin, C. "Laser-Assisted charge transfer reaction in slow ion-atom collisions: Coupled dressed quasimolecular-states approach". *J. Chem. Phys.* **1984**, *81*, 788. Last, I.; Baer, M. "Quantal and Semi-classical studies of reactions in strong laser fields: F($^2P_{1/2}$,$^2P_{3/2}$) + H_2 + $h\nu$ (0.117, 0.469, and 1.17 eV)". *J. Chem. Phys.* **1985**, *82*, 4954. Lau, A. M. F.; Dixit, S. N.; Tellinghuisen, J. "Photon-catalyzed bound-continuum processes: Post saturation fluorescence quenching and huge enhancement of fragments in I_2". *Chem. Phys. Lett.* **1984**, *105*, 567. Milfield, K. F.; Bowman, J. M. "A model study of the laser-induced stabilization of a collision complex". *CPL* **1983**, *100*, 529. Peploski, J. C.; Eno, L. "A simple model study of reactive collisions in an intense nonresonant laser field". *J. Chem. Phys.* **1985**, *83*, 2947.). Experimental observation of altered events is feasible, but interpretation of any such observations will be complicated by various multiphoton processes which are certain to occur simultaneously.
(81) Yariv, A. *Theory and Applications of Quantum Mechanics*; Wiley: New York, 1982.
(82) For collision-free transitions, especially in monochromatic molecular beams, the coherence of the radiation is important. Exact solution of the time-dependent Schrödinger equation (ref 81; Ramsey, N. F. *Molecular Beams*; Oxford University Press: London, 1955; Dyke, T. R.; Tomasevich, G. R.; Klemperer, W.; Falconer, W. E. "Electric Resonance Spectroscopy of Hypersonic Molecular Beams". *J. Chem. Phys.* **1972**, *57*, 2277) shows that at high power, the transition probability oscillates between 0 and 1 with the Rabi frequency, Ω. Equation 34 results if the source is incoherent.
(83) Collision-free ionization of rare gases has been observed in the power range 1–1000 GW/cm^2. He^{2+} is formed by a 68-photon absorption! (L'Huillier, A.; Lompre, A. L.; Mainfray, G.; Manus, C. *J. Phys.* **1983**, *B16*, 1363).
(84) Tellinghuisen, J.; Hays, A. K.; Hoffman, J. M.; Tisone, G. C. "Spectroscopic studies of diatomic noble gas halides. II. Analysis of bound-free emission from XeBr, XeI, and KrF". *J. Chem. Phys.* **1976**, *65*, 4473.
(85) Tellinghuisen, J.; Ragone, A.; Kim, M. S.; Auerbach, D. J.; Smalley, R. E.; Wharton, L.; Levy, D. H. "The dispersed fluorescence spectrum of NaAr: Ground and excited state potential curves". *J. Chem. Phys.* **1979**, *71*, 1283.
(86) Experimental intensities are in good agreement with the overlap integrals, but not necessarily with the frequently used notion that transitions occur most readily at the classical turning points of the motion. See also: Mulliken, R. S. "Role of Kinetic Energy in the Franck–Condon Principle". *J. Chem. Phys.* **1971**, *55*, 309.
(87) Richardson, W. C.; Setser, D. W.; Albritton, D. L.; Schmeltekop, A. L. "Vibrational and Rotational Excitation in He(2 $^3S_1$) Penning Ionization: Examples of Non-Vertical Processes". *Chem. Phys. Lett.* **1971**, *12*, 349.
(88) Chaquin, P.; Sevin, A.; Yu, H. *J. Phys. Chem.* **1985**, *89*, 2813.
(89) Kroll, N. M.; Watson, K. M. *Phys. Rev. A* **1976**, *A13*, 1018.
(90) (a) George, T. F.; Zimmerman, I. H.; Yuan, J. M.; Laing, J. R.; DeVries, P. L. "A New Concept in Laser-Assisted Chemistry: The Electron-Field Representation". *Acc. Chem. Res.* **1977**, *10*, 449. (b) George, T. F. "Laser Stimulated Molecular Dynamics and Rate Processes". *J. Phys. Chem.* **1982**, *86*, 10.
(91) (a) Sizer, T., II; Raymer, M. G. "Modification of Atomic Collision Dynamics by Intense Ultrashort Laser Pulses". *Phys. Rev. Lett.* **1986**, *56*, 123. (b) Sizer, T., II; Raymer, M. G., "Atomic Collisions in the Presence of Intense, Ultrashort Laser Pulses". *Phys. Rev. A* **1987**, *36*, 2643.
(92) (a) Orel, A. E.; Miller, W. H. "Collision Induced Absorption Spectra for gas phase". *J. Chem. Phys.* **1980**, *73*, 241. (b) Orel, A. E.; Miller, W. H. "Classical model for laser-induced nonadiabatic collision processes". *J. Chem. Phys.* **1980**, *72*, 5139. (c) Orel, A. E.; Miller, W. H. "Infrared laser enhancement of chemical reactions via collision induced absorption". *J. Chem. Phys.* **1979**, *70*, 4393. (d) Orel, A. E.; Miller, W. H. "Infrared laser induced chemical reactions". *Chem. Phys. Lett.* **1978**, *57*, 362.
(93) Welsh, H. L. *MTP Int. Rev. Sci., Phys. Chem., Ser. One* **1972**, *13*.
(94) Polanyi, J. C.; Wolf, R. J. "Spectroscopy of the transition state (theory) Emission from ABC‡* in A + BC → ABC‡* → AB + C*". *J. Chem. Phys.* **1981**, *75*, 5951.
(95) (a) Mayne, H. R.; Poirier, R. A.; Polanyi, J. C. "Spectroscopy of the Transition State (Theory) II: Absorption by H_3‡ in H + H_2 → H_3‡ → H_2 + H". *J. Chem. Phys.* **1984**, *80*, 4025. (b) Mayne, H. R.; Polanyi, J. C.; Sathyamurthy, N.; Raynor, S. "Spectroscopy of the Transition State (theory). 3. Absorption by H_3‡ in the 3-D reaction H + H_2". *J. Phys. Chem.* **1984**, *88*, 4064.
(96) Agrawal, P. M.; Hohan, V.; Sathyamurthy, N. "Time Dependent Wave Mechanical Study of the Wings to the Lyman-a line in H + H_2 reactive collisions". *Chem. Phys. Lett.* **1985**, *114*, 3430.
(97) Engel, V.; Schinke, R. "Transition State Spectroscopy of the Collinear H + H_2 > H_3‡ reaction". *Chem. Phys. Lett.* **1985**, *122*, 103.
(98) Engel, V.; Bacic, Z.; Schinke, R.; Shapiro, M. "Absorption spectra for collinear (non-reactive) H_3: Comparison between quantal and classical calculations". *J. Chem. Phys.* **1985**, *82*, 4844.
(99) Sinha, S.; Sathyamurthy, N.; Banerjee, K. "Absorption Spectrum for the transition State H_3‡—A quantum mechanical model study". *Proc. Indian Acad. Sci. (Chem. Sci.)* **1986**, *96*, 215.
(100) The usual nomenclature is confusing. The central portion of the atomic line is called the line *core*, and the broadening by these gentle collisions is described in the *impact* approximation. (See ref 22.)
(101) Kitsopoulos, T.; Metz, R. B.; Weaver, A.; Neumark, D. M., personal communication, 1987.
(102) Benz, A.; Morgner, H. "Transition state spectroscopy with electrons. The reaction of He (2 ^3S, 2 ^1S) with Cl_2". *Mol. Phys.* **1986**, *57*, 319.
(103) Yamashita, K.; Morokuma, K., personal communication, 1987.
(104) Dantus, M.; Rosker, M. J.; Zewail, A. H. "Real-Time Femtosecond Probing of "Transition States" in Chemical Reactions". *J. Chem. Phys.*, to be published.